Supplementary Materials:

Materials and Methods

Animals. Male C57BL/6J at 8-12 weeks of age were housed in light-tight boxes and entrained to LD12:12 conditions. After a minimum of 7 days, animals were transferred to constant darkness (DD) conditions. Thirty-six hours after DD, liver samples (N=3-6 mice) were collected every 4 hrs. All animal experiments were in accordance with guidelines of the UT Southwestern Medical Center Animal Care and Use Committee.

Antibodies. Antibodies against PER1, PER2, CLOCK, and BMAL1 were made as described previously (*7*). CRY1 antibody was made as described (*63*). CRY2 (epitope: residues 514-592) and p300 (epitope; residues 60-242 of human p300) antibodies were generated using guinea pigs (Cocalico Biological) and serum was affinity purified using the same protein used to raise antibody. NPAS2 antibody (*64*) was a kind gift from Dr. Steven McKnight (UT Southwestern Medical Center). BMAL1, CLOCK, NPAS2, PER1, PER2, CRY1, CRY2, p300 and CBP antibodies were validated by western blot analysis of liver nuclei from wild-type mice. In addition, the BMAL1, PER2, and CRY2 antibodies were validated using either liver or cerebellum tissue lysates including the appropriate knockout mouse control. The PER1 antibody was validated using mouse embryonic fibroblast (MEF) extracts derived from wild-type and *Per1* knockout mice. The CLOCK antibody was also validated using MEFs isolated from wild-type, *Bmal1* knockout and *Clock* knockout mice. P300 antibody was validated by in vitro translated protein with a full-length p300 cDNA-pcDNA3.1 or empty pcDNA3.1. RNAPII-8WG16 (MMS-126R) antibody (*50*) was purchased from Covance. RNAPII-Ser5P (clone 3E8, 04-1572) antibody (*51*) was purchased from Millipore and RNAPII-Ser5P (ab5131) antibody

(*57*) was purchased from Abcam. H3K4me1 (ab8895), H3K4me3 (ab1012), H3K9ac (ab4441), H3K27ac (ab4729), H3K36me3 (ab9050) and H3K79me2 (ab3594) antibodies were purchased from Abcam. CBP antibody was monoclonal AC238 culture supernatant (*65*).

Chromatin Immunoprecipitation Sequencing (ChIP-seq). Livers from mice (C57BL/6J) were immediately homogenized in 4 ml per liver of 1X PBS containing 1% formaldehyde. The homogenate was kept for 8 min at room temperature, 250 µl of 2.5 M glycine was added to stop the reaction on ice. For dual crosslinking (*66, 67*), livers were homogenized in 4 ml per liver of 1X PBS containing 2 mM EGS, kept for 20 min at room temperature, formaldehyde was added (final conc. 1%) for 8 min at room temperature and 250 µl of 2.5 M glycine was added to stop the reaction on ice. The homogenate was resuspended in 10 ml of ice-cold 2.3 M sucrose contacting 150 mM glycine, 10 mM HEPES pH 7.6, 15 mM KCl, 2 mM EDTA, 0.15 mM spermine, 0.5 mM spermidine, 0.5 mM DTT and 0.5 mM PMSF, and layered on top of a 3 ml cushion of 1.85 M sucrose (containing the same ingredients and including 10% glycerol) and centrifuged for 1 hr at 24,000 rpm at 4°C in a Beckman SW32.1 rotor. The nuclei were resuspended in 1 ml of 10 mM Tris pH 7.5, 150 mM NaCl, 2 mM EDTA, transferred to a 1.5 ml microfuge tube, centrifuged for 3 min at 3000 rpm at 4°C, washed again and stored at -80°C until use. The nuclei from two livers were pooled before sonication. For BMAL1 and 8WG16 antibodies, the formaldehyde-crosslinked nuclei were resuspended in 0.8 ml per liver of lysis buffer (50 mM Tris pH 7.5, 10 mM EDTA, 1% SDS, 1 mM PMSF and Roche complete EDTA free protease inhibitor cocktail) and sonicated 10 times for 30 sec at 4°C using a Covaris S2 ultrasonicator. For CLOCK and NPAS2 antibodies, the dual crosslinked nuclei were resuspended in 0.8 ml per liver of Sarkosyl lysis buffer (50 mM Tris pH 7.5, 10 mM EDTA,

0.5% *N*-lauroylsarcosine, 1 mM PMSF and Roche complete EDTA free protease inhibitor cocktail) and sonicated 6 times for 30 sec at 4°C using a Covaris S2 ultrasonicator. The fragmented chromatin was then diluted tenfold with IP buffer (10 mM Tris pH 7.5, 150 mM NaCl, 1 mM EDTA, 1% Triton X-100, 0.1% sodium deoxycholate, 1 mM PMSF, protease inhibitor cocktail). For PER1, PER2, CRY1, CRY2, CBP and p300 antibodies, the dual-crosslinked nuclei were resuspended in 3 ml per liver of IP buffer and sonicated 48 times for 5 sec on ice using a Misonix S-4000 sonicator. For RNAPII-Ser5P antibody, the formaldehyde-crosslinked nuclei were resuspended in 0.8 ml per liver of Sarkosyl lysis buffer, sonicated 6 times for 30 sec at 4°C using a Covaris S2 ultrasonicator, and diluted 10-fold with IP buffer. For H3K4me1, H3K4me3, H3K9ac, H3K27ac, H3K36me3 and H3K79me2 antibodies, the formaldehyde-crosslinked nuclei were resuspended in 0.7 ml per liver of 10mM Tris pH 7.5 and 100 mM NaCl, sonicated 5 times for 30 sec at 4°C using a Covaris S2 ultrasonicator, incubated for 40 min at 37°C with 200 kunitz units of Micrococcal Nuclease and 2 mM $CaCl_2$, and then stopped with 10 mM EGTA and 1% SDS. The digested chromatin was then diluted 10-fold with IP buffer. Approximately 120 µg (for transcription factors) or 80 µg (for histones) of fragmented chromatin was pre-cleared by incubating with 40 µl of protein A-agarose (Sigma) for 2 hr at 4°C on a rotating wheel. Pre-cleared chromatin was then incubated with antibody overnight at 4°C on a rotating wheel, 10 µl of Protein A/G Plus-agarose was then added and incubated for 1.5 hr at 4°C. Beads were then washed twice with IP buffer, twice with high salt wash buffer (20 mM Tris pH 7.5, 500 mM NaCl, 2 mM EDTA, 1% Triton X-100, 1 mM PMSF), twice with LiCl wash buffer (20 mM Tris pH 7.5, 250 mM LiCl, 2 mM EDTA, 0.5% Igepal CA-630, 1% sodium deoxycholate, 1 mM PMSF), and once with TE. Co-immunoprecipitated DNA fragments were eluted with 100 µl of 20 mM Tris pH 7.5, 5 mM EDTA, 0.5% SDS, then reverse crosslinked at

65°C for overnight, incubated with 10 μg of RNaseA for 30 min at 37°C, with 160μg of proteinase K for 30 min at 55°C, and then purified using a Qiaquick PCR purification Kit (Qiagen).

Sequencing library construction was performed as described (*68*). The immunoprecipitated DNA fragments were repaired by the End-It DNA End Repair Kit (Epicentre Biotechnology) according to the manufacturer's instructions. The end-repaired ChIP DNA fragments were purified by MinElute Reaction Cleanup Kit (Qiagen) and eluted in 20 μl in EB buffer. The resulting DNA fragments were ligated with P1 and P2 adaptors for the Applied Biosystems SOLiD system for 20 min at room temperature using the Quick Ligase Kit (NEB), followed by purification using the MinElute Reaction Cleanup Kit (Qiagen). The purified, adaptor-ligated ChIP DNA fragments were run on 5% native polyacrylamide gel electrophoresis (PAGE) for an in-gel PCR reaction. A gel slice containing 175–200 bp adaptor-ligated ChIP DNA fragments (corresponding to 115-140 bp genomic fragment sizes) was cut and shredded. PCR Platinum Supermix (100 μl, Invitrogen), 50 pmol of PCR primers with barcodes, 0.5 μl Taq DNA polymerase (NEB), and 0.15 μl p.f.u. Turbo DNA polymerase (Stratagene) were added into the shredded gel slice. The adaptor-ligated ChIP DNA fragments were amplified by 14-19 cycles of in-gel PCR. After the PCR reaction, gel pieces were filtered out with a 0.45 μm filter spin column, and the amplified ChIP-seq library was purified by the MinElute PCR purification kit (Qiagen). The library was purified by one more round of 5% PAGE. A gel slice containing 200-230 bp PCR products (110-130 bp fragment size) was cut and shredded, and the amplified library was extracted out of the gel by passive elution in elution buffer (2.5 M ammonium acetate in TE). Gel pieces were removed with a spin column, and the resulting ChIP-seq library was purified using the QIAquick PCR purification kit (Qiagen). SOLiD sequencing of ChIP-seq

libraries were performed on an Applied Biosystems SOLiD4 or 5500xl instrument with 35-bp reads according to manufacturer's instructions (Life Technologies) by the UTSW McDermott Next Generation Sequencing Core. Sequence reads were mapped to the mouse genome (NCBI m37/mm9) with Applied Biosystems BioScope v1.3. The mapping algorithm uses a seed and extend mapping scheme using the first 25 bp as the "seed" and allowing a maximum of two mismatches in the seed region for 35 bp reads. Two mapping options (ma.to.bam.output.filter=alignment_score, and ma.to.bam.clear.zone = 5) were used to indicate that the mapped reads in the ma file are limited to "unique" reads for output to the bam file. These two parameters indicate that the reads are primary and unique. Uniqueness is determined by the clear zone number. If there are two primary mapping locations for a read, the read is considered unique if the mapping quality of that mapping location is at least 5 greater than the next primary mapping location. If the score is 5 or greater, all other mappings are discarded and the higher quality mapping is kept as the unique read. Otherwise all mappings are discarded. If there is only one mapping location, that location is kept and termed unique. Duplicates were removed using Picard MarkDuplicates (http://picard.sourceforge.net).

In order to adjust for differences in sequencing depth among time samples, the sequence reads were "down sampled" to the lowest number of the uniquely mapped reads with duplicates among the six time points for each ChIP factor. In determining how best to compensate for variations in sequence depth among samples during the sequencing runs, we tested four different methods and came to the conclusion that down sampling was the best method. The other three methods involved normalizing either to the "total reads," "total mapped reads with duplicates" or "total mapped reads without duplicates." In each case, we found that some type of bias could be introduced depending on how different the sequencing depth (the number of sequence reads) was

among samples. Thus, we determined empirically that it was better to randomly sample the sequence reads in order to equalize the sequencing coverage rather than to numerically divide the sample reads by one of the three sequence read metrics above.

To validate our approach further, we calculated the percentage of the reads in the sample that were localized in the peaks. This analysis shows that less than 1-2% of the signal is usually contained in the peaks. Thus the peak height or number of peaks would account for only a very small fraction of the total, and therefore would only be influenced by the normalization procedure by a few percent. Because of this fact, our procedure is equivalent to normalizing to the "background."

% reads mapped in master peak area

	CT0	CT4	CT8	CT12	CT16	CT20	KO
BMAL1	0.6475%	0.8673%	0.9845%	0.4231%	0.1512%	0.1140%	0.0365%
CLOCK	0.2968%	0.2599%	0.3647%	0.2645%	0.1668%	0.1715%	0.0262%
NPAS2	0.1375%	0.1309%	0.2316%	0.1266%	0.0862%	0.0404%	
PER1	0.1588%	0.1342%	0.0818%	0.6136%	0.3148%	0.3998%	0.0852%
PER2	0.3617%	0.1874%	0.2356%	0.6044%	1.0179%	0.8086%	0.1962%
CRY1	1.8008%	1.8779%	0.7481%	1.3286%	0.6321%	1.4935%	0.3644%
CRY2	0.4955%	0.3102%	0.6556%	0.7370%	0.9125%	0.6339%	0.2434%
CBP	0.2976%	0.4353%	0.3634%	0.1760%	0.6501%	0.4021%	
p300	0.0650%	0.0679%	0.0865%	0.0322%	0.0361%	0.0424%	
8WG16	0.2204%	0.1998%	0.1948%	0.5559%	0.4363%	0.1291%	
Ser5P	2.3970%	2.1996%	1.3907%	0.8423%	1.2076%	1.8905%	

The total reads for each sample and the down sampled reads for each factor are shown in Table S1. Results were further analyzed using HOMER (*69*). Genome browser views were normalized to display uniquely mapped reads per 10 million uniquely mapped reads with duplicates.

ChIP-seq peak finding. The peaks were identified from uniquely mapped reads without duplicates using MACS with following parameters: genomic size = mm (1.87 Gb), shift = 60 and input chromatin samples as control data (*33*). A p-value threshold of 10^{-5} (default) and a ratio

between the ChIP-Seq tag count and λlocal of 10 (fold_enrichment threshold) was used. The false peaks called by MACS in Table S11 that repeatedly emerged from low complexity sequence were removed from further analysis. The peaks were then subdivided by PeakSplitter (*34*) with options of –valley 0.7 and –cutoff 7. To construct a master peak list from the six time points, the peaks obtained after PeakSplitter were merged, compared for overlaps and the peak with the highest summit value was chosen if the summit coordinates were within 120 bp. Figure S3 illustrates the master peak process in which MACS peaks are called, then subdivided with PeakSplitter and then compared for overlap and summit height.

The ChIP-seq peak overlaps (peak summit +/- 120bp) from the master peak lists were determined using HOMER (*69*). Chow-Ruskey diagrams (*70*) were made with R using the Vennerable package.

Whole transcriptome sequencing (RNA-seq). RNA was isolated from livers using Trizol reagent according to the manufacturer's instructions (Life Technologies). 10 μg of total RNA pooled from three mice (individual mouse RNA samples with RIN values of 8-9) was depleted of ribosomal RNAs using RiboMinus Eukaryote Kit for RNA-seq according to the manufacturer's instructions (Life Technologies). The removal of ribosomal RNAs was confirmed on a Bioanalyser Pico Chip (Agilent). Sequencing libraries were constructed using SOLiD Total RNA-seq Kit (Life Technologies) with a modification below. A total of 1 μg of rRNA-depleted total RNA was fragmented in the 30 μl of T4 PNK buffer for 18 min at 95°C and placed on ice immediately. Fragmented RNA was phosphorylated by adding 2 μl of T4 PNK and 1 mM ATP for 60 min at 37°C and purified by RiboMinus Concentration module (Life Technologies) prior to the adaptor ligation. SOLiD sequencing of libraries was performed on an

ABI SOLiD4 instrument with 50-bp reads according to manufacturer's instructions (Life Technologies) by the UTSW McDermott Next Generation Sequencing Core. Sequence reads were mapped to the mouse genome (NCBI m37/mm9) with Applied Biosystems BioScope v1.3 to create Wig and BigWig files for visualization on the UCSC Genome Browser. In the RNA-seq experiments, we did not observe obvious differences in the total amount of RNA at different time points. This is due to the great abundance of ribosomal RNAs in the samples (and this is still the case after ribosomal RNA depletion as assessed by the large number of ribosomal RNA reads in the samples). For these reasons, we used the conventional method of normalization to RPKM which does not appear to introduce bias among the time samples. For analysis with HOMER (*69*), sequence reads were mapped to the mouse genome (NCBI m37/mm9) with Bowtie (*71*) and Tophat (*72*) to create bam/sam/bed input files for HOMER because Bioscope derived bam/sam/bed files contained non-uniquely mapped low complexity sequence reads. To obtain reliable alignments, the reads with mapping quality less than 5 were removed by SAMtools (*73*). The UCSC canonical gene set (28,661 total; 21,789 with introns) was used for annotation of exons and introns. Among UCSC known canonical genes, we assumed that a gene was expressed if there were >5 reads in the gene body. To find expressed antisense transcripts, a threshold of >8 reads was used.

Quantitative PCR (qPCR). qPCR was performed with iTaq™ SYBR® Green Supermix with ROX (BioRad) using an Applied Biosystems PRISM 7900HT Sequence Detector. Primer sequences used for RNA quantification are described (*12, 74*). Primers used for ChIP DNA quantification were:

Name	Forward	Reverse
Dbp -2.4kb (upstream)	TGCCTCCTCTTCCACCCCAGG	CAAAGAGGCTGAGAATGGCCAGG
Dbp -0.4kb (promoter)	ACACCCGCATCCGATAGC	CCACTTCGGGCCAATGAG
Dbp +0.8kb (intron 1)	ATGCTCACACGGTGCAGACA	CTGCTCAGGCACATTCCTCAT
Dbp +2.4kb (intron 2)	TGGGACGCCTGGGTACAC	GGGAATGTGCAGCACTGGTT
Dbp +4.4kb (exon 4)	AAGAACAATGAAGCAGCCAAGAG	GGCAGCCCGCACAGATAT
Per2 -4.5kb	CCACACGGTACTCAGCGGGC	GGGTCACTGCGAGCCTTGCC
Per2E2	GGTTCCGCCCCGCCAGTATGC	CCGTCACTTGGTGCGCTCGGC
Per1E1	AGCCAGCCTGCACGTGTTCC	CAGAGACAACCCCGCCCTGC
Per1E5	CAGCACCCAAGTCCACGTG	CCGGTTGGCTAAGGATCTCTT

Time Series Analysis for Circadian Cycling. RNA cycling was assessed by three programs, COSOPT (*35*) JTK cycle (*75*) and ARSER (*76*) with expression level cutoffs, >0.05 RPKM for intron, >0.5 RPKM for exon and >0.0625 RPKM for antisense. For COSOPT and JTK cycle analyses, data was detrended by linear regression. A cycling gene was considered if two out of three programs detected cycling with threshold of $p<0.05$. The period and phase from ARSER were used for further analysis. For ChIP-seq peak analysis, two cycles were concatenated and the cycling was analyzed with ARSER ($p<0.05$).

Gene Ontology analysis. WebGestalt (*77, 78*) was used for KEGG pathway and gene ontology analyses.

Immunoblotting and Immunoprecipitation. Immunoblotting was performed as described previously (*79*). Immunoprecipitation was performed as described previously (*12*). Briefly tissues were homogenized in EB (20 mM HEPES pH 7.5, 100 mM NaCl, 0.05% TritonX-100, 1 mM EDTA, 20 mM NaF, 1 mM Na_3OV_4, Complete Mini protease inhibitor cocktail, Roche) and centrifuged at maximum speed for 10 min at 4°C. The supernatants were transferred to fresh

tubes and incubated with 1.5 μg of antibodies for 2 hr at 4°C. Ten microliters of 50% protein-A slurry (GE Healthcare Life Sciences) was added, and the incubation continued for an additional 1.5 hr. Supernatants were discarded after centrifugation at 3000 rpm at 4°C for 1 min, and protein-A beads were washed three times with 1 ml EB. Pellets were resuspended in 20 μl of 2 X SDS sample buffer and boiled for 3 min. Protein samples were separated by 10% or 6% SDS-PAGE and then transferred to a nitrocellulose membrane (Dupont NEN).

Supplemental figure legends

Fig. S1. Rhythmic DNA binding of core clock proteins, RNA polymerase and histone modifications measured by chromatin immunoprecipitation and qPCR (ChIP-qPCR). (**A**) Circadian DNA binding of BMAL1 (a), CLOCK (b), NPAS2 (c), PER1 (d), PER2 (e), CRY1 (f) and CRY2 (g). ChIP-qPCR values are shown relative to input DNA. Rhythmic DNA binding of core clock proteins is seen at E-boxes at the *Dbp* promoter (-0.4 kb), intron 1 (+0.8 kb), intron 2 (+2.4 kb), *Per2* promoter (E2) and *Per1* promoter (E1 and E5). (**B**) Temporal profiles of CBP (a), p300 (b) and RNA polymerase II (c and d). (**C**) Temporal profiles of H3K4me1 (a) H3K4me3 (b), H3K9ac (c), H3K36me3 (d), H3K79me2 (e) and H3K27ac (f) histone modifications in *Dbp*, *Per2* and *Per1* loci.

Fig. S2. UCSC genome browser view of BMAL1 ChIP-seq for two complete circadian cycles in constant darkness at the *Per1* (**A**), *Dbp* (**B**) and *Nr1d1* (**C**) loci.

Fig. S3. Illustration of ChIP-seq peak finding and master peak list construction. ChIP-seq peaks at the *Per1* (**A**), *Dbp* (**B**) and *Nr1d1* (**C**) loci. Peaks determined by MACS (*33*) are shown in orange and peaks subdivided by Peaksplitter (*34*) are shown in green. MACS peaks with fold enrichment less than 10 were filtered out. MACS peaks were then subdivided with Peaksplitter and small peaks (peak height <7) were removed. Master peaks indicated in red were chosen from the Peaksplitter peaks by combining all peaks from all 6 time points that had summit locations within 120 bp and then selecting the highest peak for the master peak list. The numbers to the left of the bars under the peaks are the tag counts (not fold enrichment) for MACS peaks (orange) or peak height for Peaksplitter peaks (green) and master peaks (red).

Fig. S4. (**A**) Genomic annotation of the binding sites for BMAL1, CLOCK, NPAS2, PER1, PER2, CRY1, CRY2, CBP, p300, RNAPII-8WG16, and RNAPII-Ser5P. The peaks were annotated to promoter-TSS (-1kb to +100bp from TSS), 5'UTR, exon, intron, 3'UTR, TTS (from TTS to +1kb) as indicated. (**B**) Overlap of BMAL1 peaks from Rey et al. (*28*) with this paper. **C**) Overlap of REV-ERBα/β peaks from Cho et al. (*30*) with circadian transcription factors and CBP from this paper.

Fig. S5. Sequence motifs of the circadian transcriptional regulators, co-activators and RNAPII binding sites in Fig. 1, 3 and 4. De novo sequence motif analysis was carried out with +/- 60 bp DNA sequence from the master peak binding sites by HOMER (*69*).

Fig. S6. (**A**) Binding coverage profiles for BMAL1 (blue), CLOCK (green), CRY1 (red), CRY2 (purple), PER1 (orange) and PER2 (brown) from -260 to +260 bp surrounding the 1444 common binding sites. (**B** and **C**) Chow-Ruskey diagrams showing circadian time dependent overlap of activator (**B**) and repressor (**C**) binding sites. MACS derived-peaks from each time point were used to determine if there is more than 1bp overlap in the peak areas. The master peak list for each factor was used to filter out false positive peaks from the MACS peak calls at each time point.

Fig. S7. Sequence motifs of the 6-way common circadian transcriptional regulators sites or the indicated unique/combination binding sites in Fig. 1D. De novo sequence motif analysis was carried out with +/- 60 bp DNA sequence from the master peak binding sites by HOMER (*69*).

Fig. S8. Comparison of temporal RNA expression profiles using qPCR, intron RNA-seq and exon RNA-seq analysis. The intron RNA (red) and exon RNA (green) expression levels are indicated on the left and right Y-axis, respectively. The highest RNA abundance measured by qPCR (blue) is normalized to highest abundance from exon reads.

Fig. S9. UCSC genome browser views of CRY1 and RNAPII-Ser5P common binding sites at the *Nr1d1* (**A**), *Nfil3* (**B**), *Adck3* (**C**) and *Ppp1r3c* (**D**) loci. Tracks for BMAL1, CLOCK, NPAS2, PER1, PER2, CRY1, CRY2, RNAPII-8WG16, RNAPII-Ser5P, CBP and p300 ChIP-seq as well as RNA-seq data are shown as indicated. In addition, tracks for REV-ERBα (NR1D1) and REV-ERBβ (NR1D2) ChIP-seq at ZT8 are shown in red for comparison (*30*). The intron RNA cycling genes (~300 genes) that peak between CT20 and CT4 are similar to those seen in fig. S7B-D and account for majority of the RNAPII-Ser5P signal that peaks at CT0.

Fig. S10. (**A**) Heat map view of 24 hr (left) and 12 hr (right) cycling DNA binding sites for CBP. Histograms of the phase of the rhythms in each class are shown below the heat map (mean circular phase is shown in red). (**B**) Heat map view of 24 hr (left) and 12 hr (right) cycling DNA binding sites for CRY1. Histograms of the phase of the rhythms in each class are shown below the heat map (mean circular phase is shown in red). (**C**) Overlap of RNAPII-Ser5P with CRY1 peaks.

Fig. S11. Temporal variation in RNAPII occupancy and histone modifications. Gene model plots for RNAPII-8WG16, RNAPII-Ser5P, H3K4me1, H3K4me3, H3K9ac, H3K27ac, H3K36me3

and H3K79me2 occupancy. The average signal from ChIP-seq from 12,680 expressed genes (top), 8945 unexpressed genes (middle) and 1371 intron cycling genes (bottom) are shown as indicated. The intron-less genes were filtered out from the analysis. Signal from all genes were normalized to a standard 40 kb gene body length for display in addition to the signal from 10 kb upstream of the TSS to 10 kb downstream of the transcription termination site (TTS) are shown in the gene model. Colors indicate the circadian time (CT) of the sample.

Fig. S12. Overlap of chromatin marks with RNAPII as a function of the circadian cycle and circadian rhythms in histone modifications at promoter and enhancer sites. (**A**) Chow-Ruskey diagrams showing the overlap of RNAPII binding and histone modifications at six circadian times. The gene body +/- 1 kb was used to determine if the gene was positive for RNAPII-8WG16 occupancy, and/or H3K4me4, H3K9ac or H3K27ac modifications. (**B** and **C**) ChIP-seq binding profiles at promoter and intergenic sites. Average signal from -2 kb to +2 kb of BMAL1 (**B**) or CBP binding sites (**C**) in promoter or intergenic sites are plotted as indicated.

Fig. S13. UCSC genome browser views of BMAL1, CLOCK, NPAS2, PER1, PER2, CRY1, CRY2, RNAPII-8WG16, RNAPII-Ser5P, CBP, p300, H3K4me1, H3K4me3, H3K9ac, H3K27ac, H3K36me3 and H3K79me2 ChIP-seq as well as RNA-seq data are shown as indicated at: (**A**) *Nr1d1* (*Rev-erbα*); (**B**) *Nr1d2* (*Rev-erbβ*); (**C**) *Dbp*; (**D**) *Nfil3* (*E4BP4*); (**E**) *Per1*; (**F**) *Per2*; (**G**) *Per3*; (**H**) *Cry1*; (**I**) *Cry2*; (**J**) *Gm129*; (**K**) *Hlf*; (**L**) *Tef*; (**M**) *Bhlhe40* (*Dec1*); (**N**) *Bhlhe41* (*Dec2*).

Supplemental Tables.

Table S1. Sequence statistics for ChIP-seq and RNA-seq experiments showing the number of runs, the reads per sample and the results of normalization by down sampling. The run listed at the top of each category is the experiment illustrated in this paper. Replicate experiments are shown below.

Table S2. Master peak lists for ChIP-seq experiments for BMAL1, CLOCK, NPAS2, PER1, PER2, CRY1, CRY2, CBP, p300, RNAPII-8WG16, and RNAPII-Ser5P ranked by the average tag count across all 6 times points.

Table S3. Gene ontology analysis for BMAL1, CLOCK, NPAS2, PER1, PER2, CRY1, CRY2, CBP, p300 and RNAPII-8WG16 ChIP-seq experiments.

Table S4. KEGG pathway analysis for BMAL1, CLOCK, NPAS2, PER1, PER2, CRY1, CRY2, CBP, p300 and RNAPII-8WG16 ChIP-seq experiments.

Table S5. List of the genes with cycling antisense RNA transcripts.

Table S6. List of cycling intron RNA genes.

Table S7. List of cycling exon RNA genes.

Table S8. Gene ontology analysis of the intron or exon cycling genes.

Table S9. KEGG pathway analysis of the intron or exon cycling genes.

Table S10. The majority of genes bound by circadian transcriptional regulators (CTR), co-activators and RNAPII are expressed.

Table S11. List of false positive peaks removed from the ChIP-seq peaks.

Fig. S1

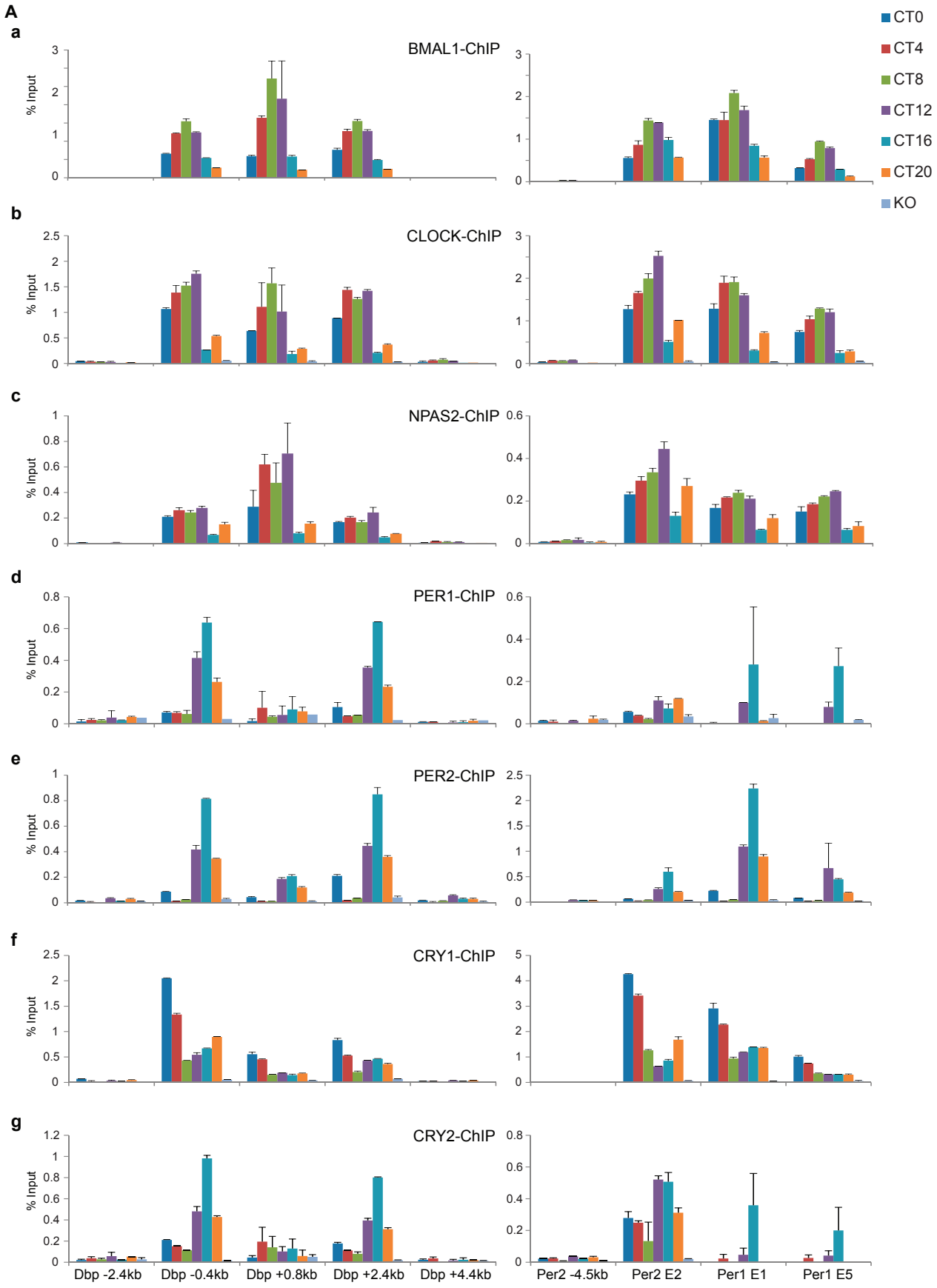
A
a
BMAL1-ChIP
b
CLOCK-ChIP
c
NPAS2-ChIP
d
PER1-ChIP
e
PER2-ChIP
f
CRY1-ChIP
g
CRY2-ChIP
% Input
CT0
CT4
CT8
CT12
CT16
CT20
KO
Dbp -2.4kb
Dbp -0.4kb
Dbp +0.8kb
Dbp +2.4kb
Dbp +4.4kb
Per2 -4.5kb
Per2 E2
Per1 E1
Per1 E5

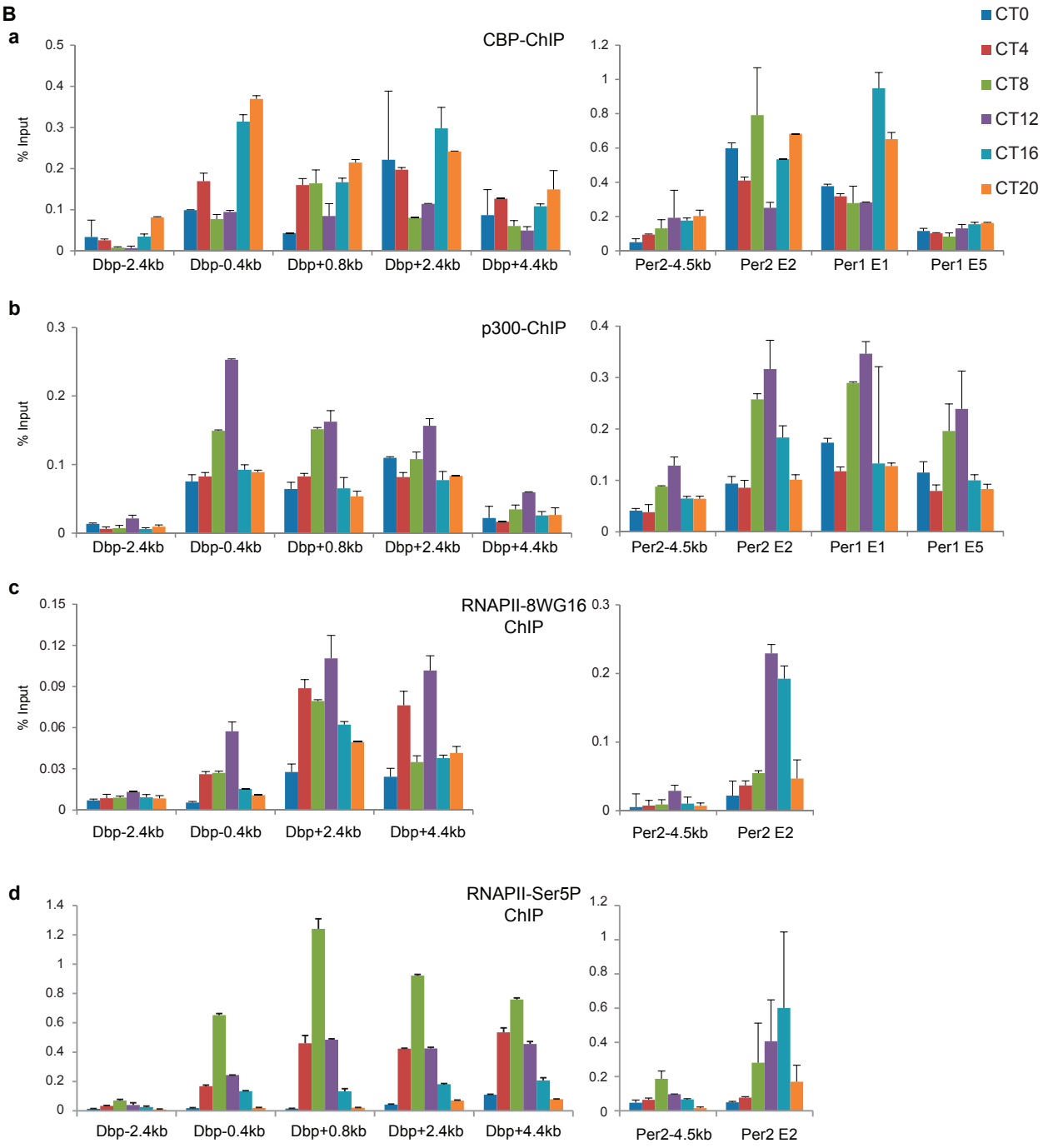
B
a
CBP-ChIP
% Input
0.5
0.4
0.3
0.2
0.1
0
Dbp-2.4kb
Dbp-0.4kb
Dbp+0.8kb
Dbp+2.4kb
Dbp+4.4kb
1.2
1
0.8
0.6
0.4
0.2
0
Per2-4.5kb
Per2 E2
Per1 E1
Per1 E5
CT0
CT4
CT8
CT12
CT16
CT20
b
p300-ChIP
% Input
0.3
0.2
0.1
0
Dbp-2.4kb
Dbp-0.4kb
Dbp+0.8kb
Dbp+2.4kb
Dbp+4.4kb
0.4
0.3
0.2
0.1
0
Per2-4.5kb
Per2 E2
Per1 E1
Per1 E5
c
RNAPII-8WG16 ChIP
% Input
0.15
0.12
0.09
0.06
0.03
0
Dbp-2.4kb
Dbp-0.4kb
Dbp+2.4kb
Dbp+4.4kb
0.3
0.2
0.1
0
Per2-4.5kb
Per2 E2
d
RNAPII-Ser5P ChIP
1.4
1.2
1
0.8
0.6
0.4
0.2
0
Dbp-2.4kb
Dbp-0.4kb
Dbp+0.8kb
Dbp+2.4kb
Dbp+4.4kb
1.2
1
0.8
0.6
0.4
0.2
0
Per2-4.5kb
Per2 E2

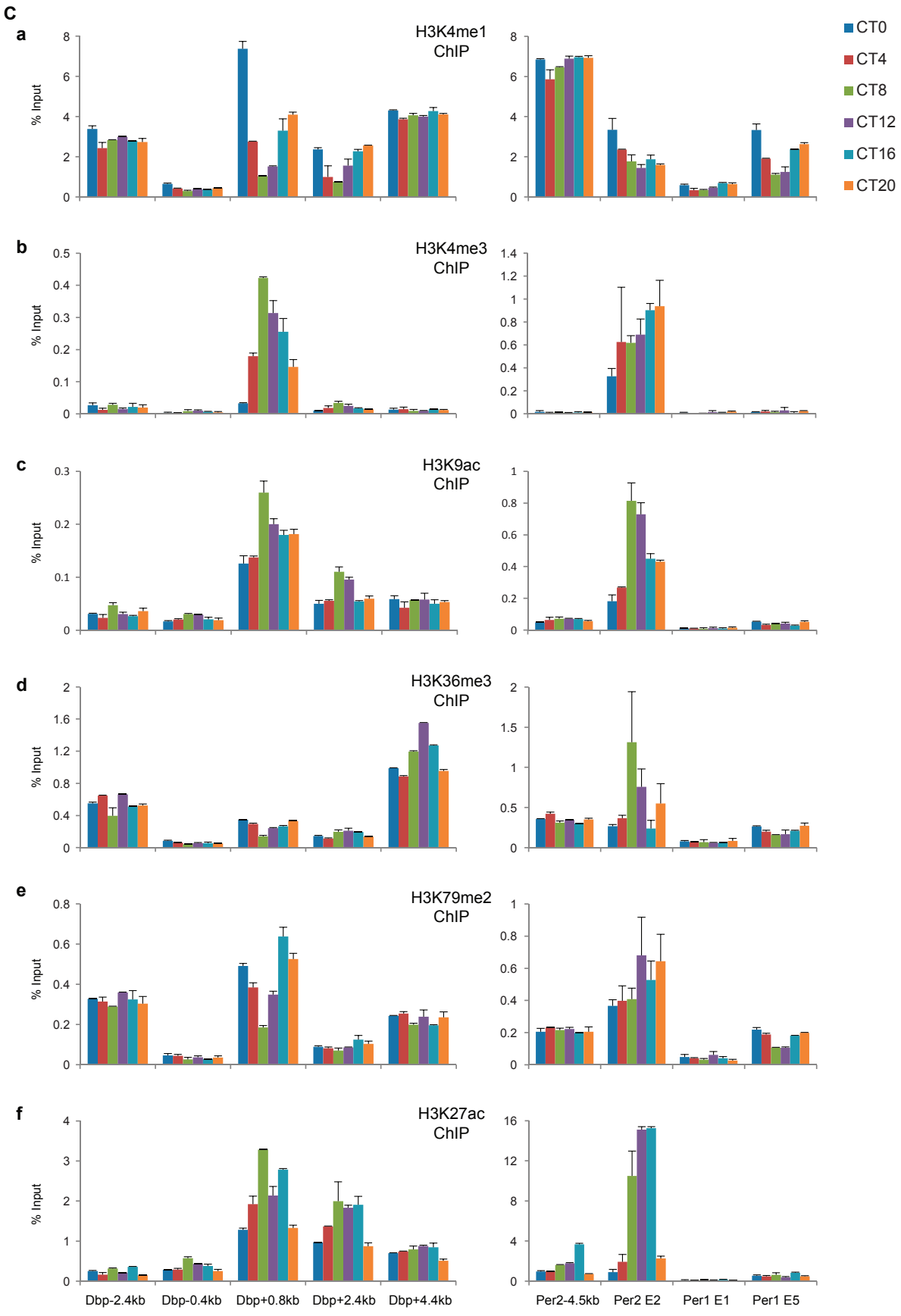
C
a
H3K4me1
ChIP
% Input
b
H3K4me3
ChIP
% Input
c
H3K9ac
ChIP
% Input
d
H3K36me3
ChIP
% Input
e
H3K79me2
ChIP
% Input
f
H3K27ac
ChIP
% Input
CT0
CT4
CT8
CT12
CT16
CT20
Dbp-2.4kb
Dbp-0.4kb
Dbp+0.8kb
Dbp+2.4kb
Dbp+4.4kb
Per2-4.5kb
Per2 E2
Per1 E1
Per1 E5

Fig. S2


A
Scale
chr11:
5 kb
mm9
68910000
68915000
68920000
BMAL1_CT00
BMAL1_CT04
BMAL1_CT08
BMAL1_CT12
BMAL1_CT16
BMAL1_CT20
BMAL1_CT24
BMAL1_CT28
BMAL1_CT32
BMAL1_CT36
BMAL1_CT40
BMAL1_CT44
BMAL1_KO
UCSC Genes
Per1
Mammal Cons
B
Scale
chr7:
2 kb
mm9
52959000
52960000
52961000
52962000
52963000
52964000
52965000
52966000
52967000
52968000
BMAL1_CT00
BMAL1_CT04
BMAL1_CT08
BMAL1_CT12
BMAL1_CT16
BMAL1_CT20
BMAL1_CT24
BMAL1_CT28
BMAL1_CT32
BMAL1_CT36
BMAL1_CT40
BMAL1_CT44
BMAL1_KO
UCSC Genes
Car11
Dbp
Sphk2
Mammal Cons
C
Scale
chr11:
10 kb
mm9
98635000
98640000
98645000
BMAL1_CT00
BMAL1_CT04
BMAL1_CT08
BMAL1_CT12
BMAL1_CT16
BMAL1_CT20
BMAL1_CT24
BMAL1_CT28
BMAL1_CT32
BMAL1_CT36
BMAL1_CT40
BMAL1_CT44
BMAL1_KO
UCSC Genes
Thra
Nr1d1
Mammal Cons

Fig. S3

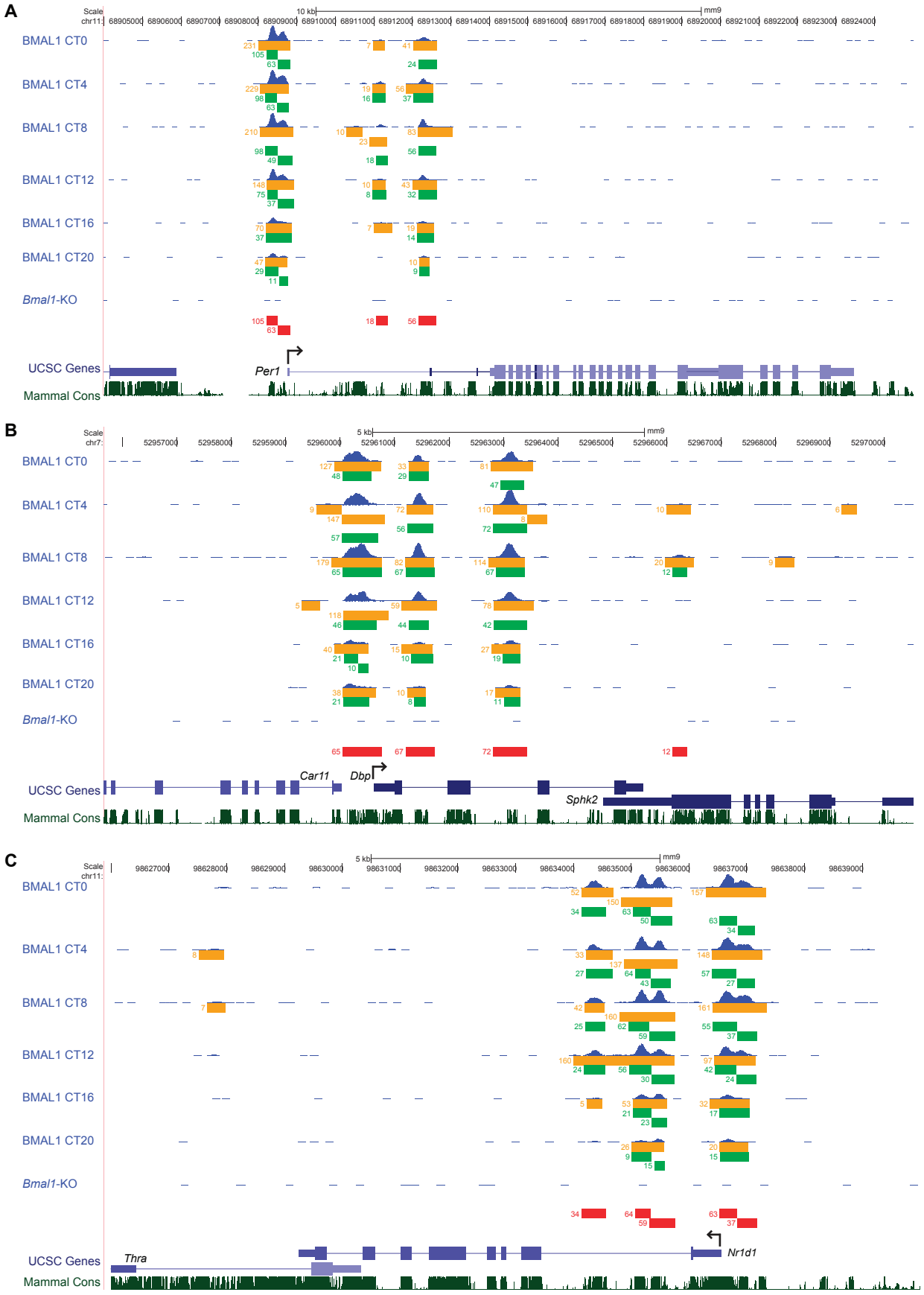
A
Scale
chr11:
10 kb
mm9
BMAL1 CT0
BMAL1 CT4
BMAL1 CT8
BMAL1 CT12
BMAL1 CT16
BMAL1 CT20
Bmal1-KO
UCSC Genes
Per1
Mammal Cons
B
Scale
chr7:
5 kb
mm9
BMAL1 CT0
BMAL1 CT4
BMAL1 CT8
BMAL1 CT12
BMAL1 CT16
BMAL1 CT20
Bmal1-KO
Car11
Dbp
Sphk2
UCSC Genes
Mammal Cons
C
Scale
chr11:
5 kb
mm9
BMAL1 CT0
BMAL1 CT4
BMAL1 CT8
BMAL1 CT12
BMAL1 CT16
BMAL1 CT20
Bmal1-KO
Thra
Nr1d1
UCSC Genes
Mammal Cons

Fig. S4

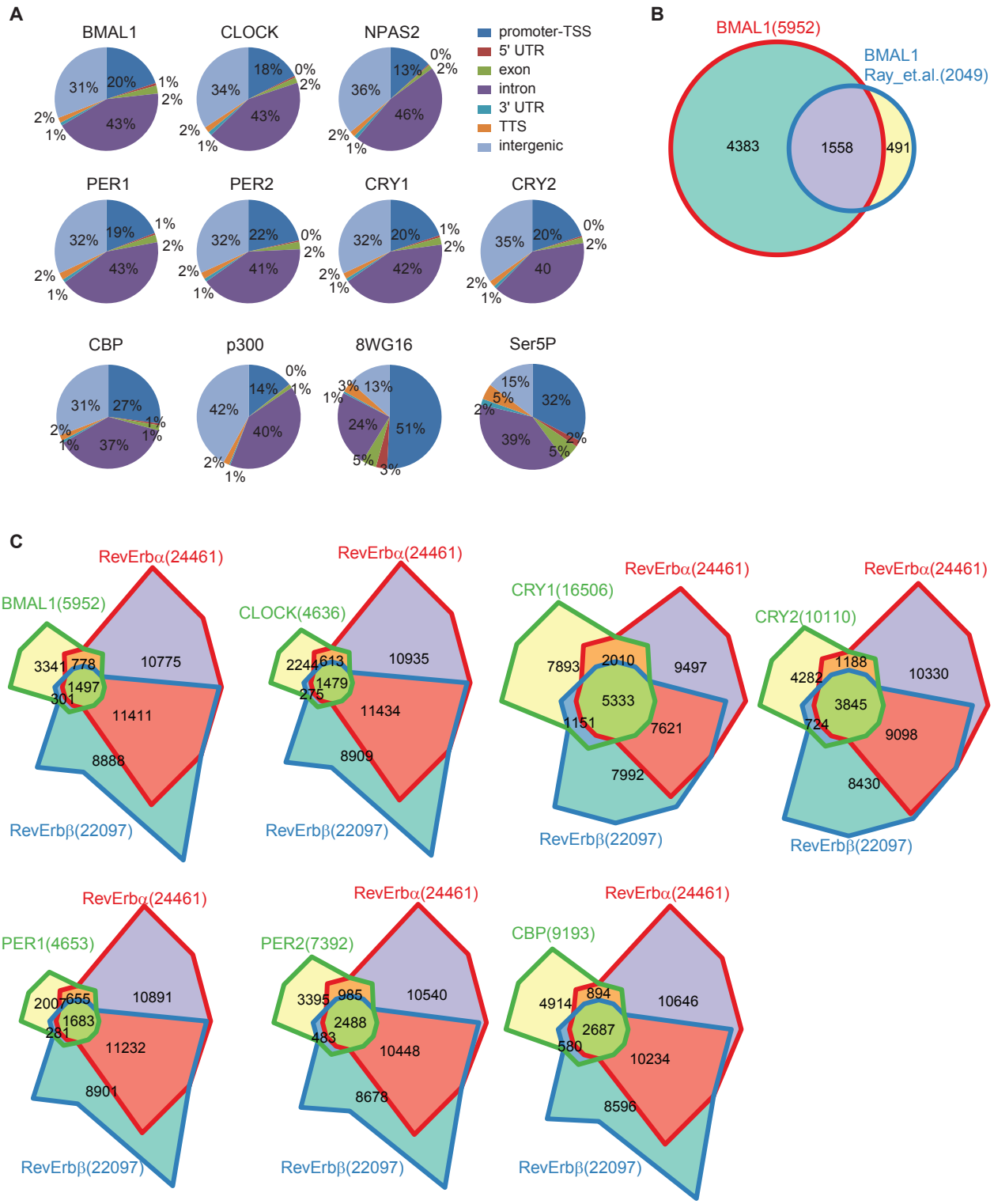
A
BMAL1
CLOCK
NPAS2
PER1
PER2
CRY1
CRY2
CBP
p300
8WG16
Ser5P
promoter-TSS
5' UTR
exon
intron
3' UTR
TTS
intergenic
B
BMAL1(5952)
BMAL1
Ray_et.al.(2049)
4383
1558
491
C
RevErbα(24461)
BMAL1(5952)
RevErbβ(22097)
CLOCK(4636)
CRY1(16506)
CRY2(10110)
PER1(4653)
PER2(7392)
CBP(9193)

Fig. S5

BMAL1	P-value	% of Targets	Best Match/Details
	1e-1929	61.88%	Mycn
	1e-265	9.49%	bZIP_cEBP-like_subclass
	1e-172	20.82%	Erra(NR)
	1e-153	28.29%	HNF6
	1e-134	7.39%	INO2
	1e-120	14.43%	fkh
	1e-87	28.44%	NF1-halfsite(CTF)
	1e-76	14.40%	ARG81
	1e-58	8.79%	GC-box
	1e-46	1.44%	HNF1A
	1e-43	3.63%	RXR(NR/DR1)
	1e-35	9.86%	Zfp105_2
	1e-35	1.53%	HNF4a
	1e-16	0.39%	Mafk_2
	1e-13	0.69%	Arnt::Ahr

CLOCK	P-value	% of Targets	Best Match/Details
	1e-1024	38.76%	MAX
	1e-440	14.52%	bZIP_cEBP-like_subclass
	1e-212	21.18%	Erra(NR)
	1e-137	13.18%	Foxa2(Forkhead)
	1e-79	22.41%	Nuclear_Receptor_class
	1e-71	20.71%	NF1-halfsite(CTF)
	1e-59	5.18%	HNF6(Homeobox)
	1e-54	11.26%	GC-box
	1e-54	4.18%	HNF1A
	1e-49	8.24%	FXR(NR/IR1)
	1e-19	12.68%	SCL
	1e-17	0.43%	fkh

NPAS2	P-value	% of Targets	Best Match/Details
	1e-447	46.63%	TYE7
	1e-272	18.34%	NFIL3
	1e-115	29.39%	Erra(NR)
	1e-72	18.93%	FKH2
	1e-49	44.52%	NFIC
	1e-48	39.43%	hth
	1e-36	4.07%	HNF1A
	1e-22	23.04%	Ddit3::Cebpa
	1e-19	5.21%	p53
	1e-14	3.01%	Forkhead_class
	1e-13	2.37%	HNF6(Homeobox)

PER1	P-value	% of Targets	Best Match/Details
	1e-562	50.20%	Arnt
	1e-373	23.68%	bZIP_cEBP-like_subclass
	1e-205	31.31%	Erra(NR)
	1e-191	18.81%	FOXA1
	1e-182	9.03%	HNF6
	1e-133	42.47%	NFIC
	1e-118	47.26%	vis
	1e-74	11.69%	Sp1
	1e-35	28.86%	GLN3
	1e-23	3.22%	Antp
	1e-18	2.06%	TEC1
	1e-13	2.00%	MAC1

PER2	P-value	% of Targets	Best Match/Details
	1e-704	36.99%	Mycn
	1e-563	21.05%	bZIP_cEBP-like_subclass
	1e-325	26.98%	Foxa2
	1e-276	20.17%	Erra(NR)
	1e-192	5.63%	HNF6
	1e-188	31.62%	NF1-halfsite
	1e-166	50.69%	Gsc
	1e-150	11.49%	GC-box
	1e-61	11.80%	Hnf4a_2
	1e-36	4.53%	Arnt::Ahr
	1e-24	4.26%	Nr2f2_2
	1e-14	0.57%	GFY

CRY1	P-value	% of Targets	Best Match/Details
	1e-1159	27.86%	USF1(HLH)
	1e-943	19.97%	CEBPA
	1e-903	23.09%	Erra(NR)
	1e-606	21.48%	Foxa2(Forkhead)
	1e-322	44.77%	NFIC
	1e-206	3.75%	HNF1A
	1e-185	10.86%	GC-box
	1e-153	34.90%	ECM23
	1e-135	8.45%	FXR(NR/IR1)
	1e-130	1.85%	Hnf4a_2
	1e-104	1.34%	HNF6(Homeobox)
	1e-65	10.06%	RDR1
	1e-43	6.09%	GATA3(Zf)
	1e-43	0.32%	Homeobox_class
	1e-42	1.28%	GFY(?)
	1e-20	1.46%	Trl

CRY2	P-value	% of Targets	Best Match/Details
	1e-764	21.61%	CEBPA
	1e-569	27.96%	Erra(NR)
	1e-421	23.43%	Mycn
	1e-381	32.01%	HCM1
	1e-285	47.36%	NFIC
	1e-160	12.39%	HNF6(Homeobox)
	1e-154	14.64%	GC-box
	1e-49	2.30%	HAT5
	1e-47	5.52%	NFY(CCAAT)
	1e-39	28.25%	Nuclear_Receptor_class
	1e-36	10.07%	GATA3(Zf)
	1e-31	7.94%	STE12
	1e-22	1.54%	btd
	1e-20	0.45%	GFY(?)
	1e-20	0.86%	Ddit3::Cebpa
	1e-18	0.23%	PUT3
	1e-16	6.48%	HAL9

CBP	P-value	% of Targets	Best Match/Details
	1e-663	27.58%	Erra(NR)
	1e-583	20.40%	bZIP_cEBP-like_subclass
	1e-563	39.93%	bZIP_CREB/Gbox-like_subclass
	1e-270	15.70%	FOXA1(forkhead)
	1e-229	17.92%	NFY (CCAAT)
	1e-154	16.36%	GC-box
	1e-127	7.30%	Trl
	1e-99	6.12%	GABPA
	1e-90	26.16%	NFIC
	1e-78	2.07%	HNF1B
	1e-50	1.33%	GFY(?)
	1e-47	0.56%	Pax2
	1e-40	3.23%	MBP1
	1e-19	0.77%	SUT2
	1e-13	0.18%	ct
	1e-12	0.24%	CUP9

p300	P-value	% of Targets	Best Match/Details
	1e-189	51.53%	Erra(NR)
	1e-151	30.19%	bZIP_cEBP-like_subclass
	1e-62	18.94%	fkh
	1e-41	40.53%	Hnf4a_1
	1e-38	12.32%	CCAAT-box
	1e-31	20.93%	Klf4
	1e-18	13.90%	AR-halfsite(NR)
	1e-15	53.93%	NF1-halfsite(CTF)
	1e-14	1.82%	Mybl1_1

8WG16	P-value	% of Targets	Best Match/Details
	1e-89	12.84%	GABPA
	1e-54	4.05%	YY1
	1e-32	29.06%	CHA4
	1e-30	4.66%	ELK1
	1e-29	4.43%	NRF1(NRF)
	1e-29	28.98%	HAP1
	1e-29	45.21%	ovo
	1e-26	1.03%	GFX
	1e-21	11.71%	STB5
	1e-20	2.34%	ZNF143|STAF(Zf)
	1e-18	8.40%	DCE_S_III
	1e-17	12.39%	IRC900814_1
	1e-17	15.40%	EDS1
	1e-15	5.21%	HAP4
	1e-15	0.61%	HNF1A
	1e-13	1.90%	Nkx2-5
	1e-12	3.63%	CEBP(bZIP)

Fig. S6

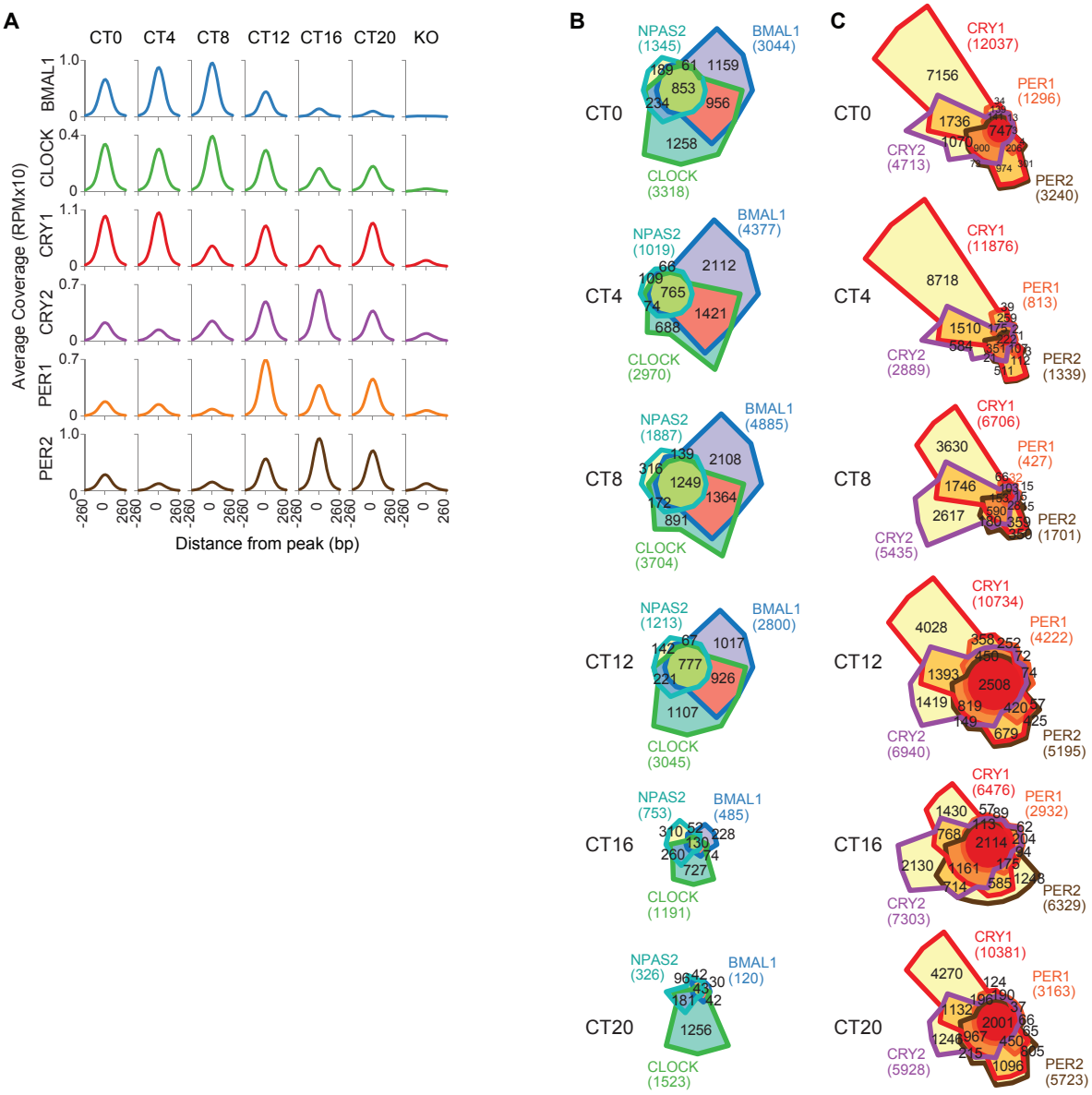
A
CT0
CT4
CT8
CT12
CT16
CT20
KO
BMAL1
CLOCK
CRY1
CRY2
PER1
PER2
Average Coverage (RPMx10)
Distance from peak (bp)
B
NPAS2 (1345)
BMAL1 (3044)
CLOCK (3318)
NPAS2 (1019)
BMAL1 (4377)
CLOCK (2970)
NPAS2 (1887)
BMAL1 (4885)
CLOCK (3704)
NPAS2 (1213)
BMAL1 (2800)
CLOCK (3045)
NPAS2 (753)
BMAL1 (485)
CLOCK (1191)
NPAS2 (326)
BMAL1 (120)
CLOCK (1523)
C
CRY1 (12037)
PER1 (1296)
CRY2 (4713)
PER2 (3240)
CRY1 (11876)
PER1 (813)
CRY2 (2889)
PER2 (1339)
CRY1 (6706)
PER1 (427)
CRY2 (5435)
PER2 (1701)
CRY1 (10734)
PER1 (4222)
CRY2 (6940)
PER2 (5195)
CRY1 (6476)
PER1 (2932)
CRY2 (7303)
PER2 (6329)
CRY1 (10381)
PER1 (3163)
CRY2 (5928)
PER2 (5723)

Fig. S7

common binding sites	P-value	% of Targets	Best Match
	1e-419	66.07%	USF1(HLH)
	1e-126	23.96%	CEBPA
	1e-80	25.21%	Erra(NR)
	1e-60	63.71%	Rfx4
	1e-55	9.07%	HNF6(Homeobox)
	1e-46	46.12%	NF1-halfsite(CTF)
	1e-42	40.24%	Forkhead_class
	1e-26	4.36%	RXR(NR/DR1)
	1e-17	24.24%	Ddit3::Cebpa
	1e-15	2.70%	TEAD1
	1e-15	13.02%	GC-box

BMAL1	P-value	% of Targets	Best Match
	1e-251	46.39%	Mycn
	1e-19	6.68%	bZIP_cEBP-like_subclass
	1e-17	20.32%	Hand1::Tcfe2a
	1e-17	7.09%	onecut

PER2	P-value	% of Targets	Best Match
	1e-43	10.45%	HNF6(Homeobox)
	1e-40	19.12%	bZIP_cEBP-like_subclass
	1e-29	26.27%	Nur77(NR)
	1e-26	10.32%	FOXA1(Forkhead)
	1e-19	22.70%	ref-1
	1e-14	4.13%	HNF4A
	1e-13	6.19%	HNF4a(NR/DR1)
	1e-13	26.82%	Nr2f2_2
	1e-12	9.77%	Sp1(Zf)

PER1/PER2/CRY1/CRY2	P-value	% of Targets	Best Match
	1e-86	27.12%	bZIP_cEBP-like_subclass
	1e-49	29.28%	Foxa2
	1e-44	59.70%	hlh-26
	1e-31	15.84%	Erra(NR)
	1e-25	24.59%	NF1-halfsite(CTF)
	1e-23	13.81%	GC-box
	1e-21	27.50%	FKH2
	1e-16	3.68%	HNF4A
	1e-16	2.41%	SPT23
	1e-13	3.42%	NFYA
	1e-12	8.75%	INO4

CRY1	P-value	% of Targets	Best Match
	1e-379	28.56%	Erra(NR)
	1e-262	20.65%	CEBPA
	1e-196	16.76%	Mycn
	1e-190	22.13%	Forkhead_class
	1e-103	54.75%	Rfx4_2
	1e-99	42.94%	NFIC
	1e-82	4.03%	HNF6(Homeobox)
	1e-59	10.63%	GC-box
	1e-34	3.78%	ELF1(ETS)
	1e-25	5.05%	FXR(NR/IR1)
	1e-14	3.80%	Trl
	1e-13	0.67%	GFY(?)
	1e-12	0.32%	Arid5a_1

CRY2	P-value	% of Targets	Best Match
	1e-150	18.08%	CEBPA
	1e-137	32.39%	Erra(NR)
	1e-63	30.47%	NFY(CCAAT)
	1e-39	10.33%	GC-box
	1e-34	6.34%	FOXA1(Forkhead)
	1e-27	6.85%	ELK4
	1e-26	7.46%	ATHB-5
	1e-21	10.38%	RIM101
	1e-17	1.17%	CTCF
	1e-15	0.47%	SNT2
	1e-13	4.32%	CRE(bZIP)
	1e-13	1.31%	fkh

CRY1/CRY2	P-value	% of Targets	Best Match
	1e-171	22.05%	CEBPA
	1e-161	41.92%	Erra(NR)
	1e-96	24.71%	FOXA1(Forkhead)
	1e-47	6.80%	HNF6(Homeobox)
	1e-46	50.19%	exd
	1e-44	51.88%	NFIC
	1e-33	6.86%	Hnf1(Homeobox)
	1e-23	7.19%	GC-box
	1e-14	15.02%	EBF1(EBF)
	1e-13	1.58%	YBR239C
	1e-13	2.78%	SKN7

Fig. S8

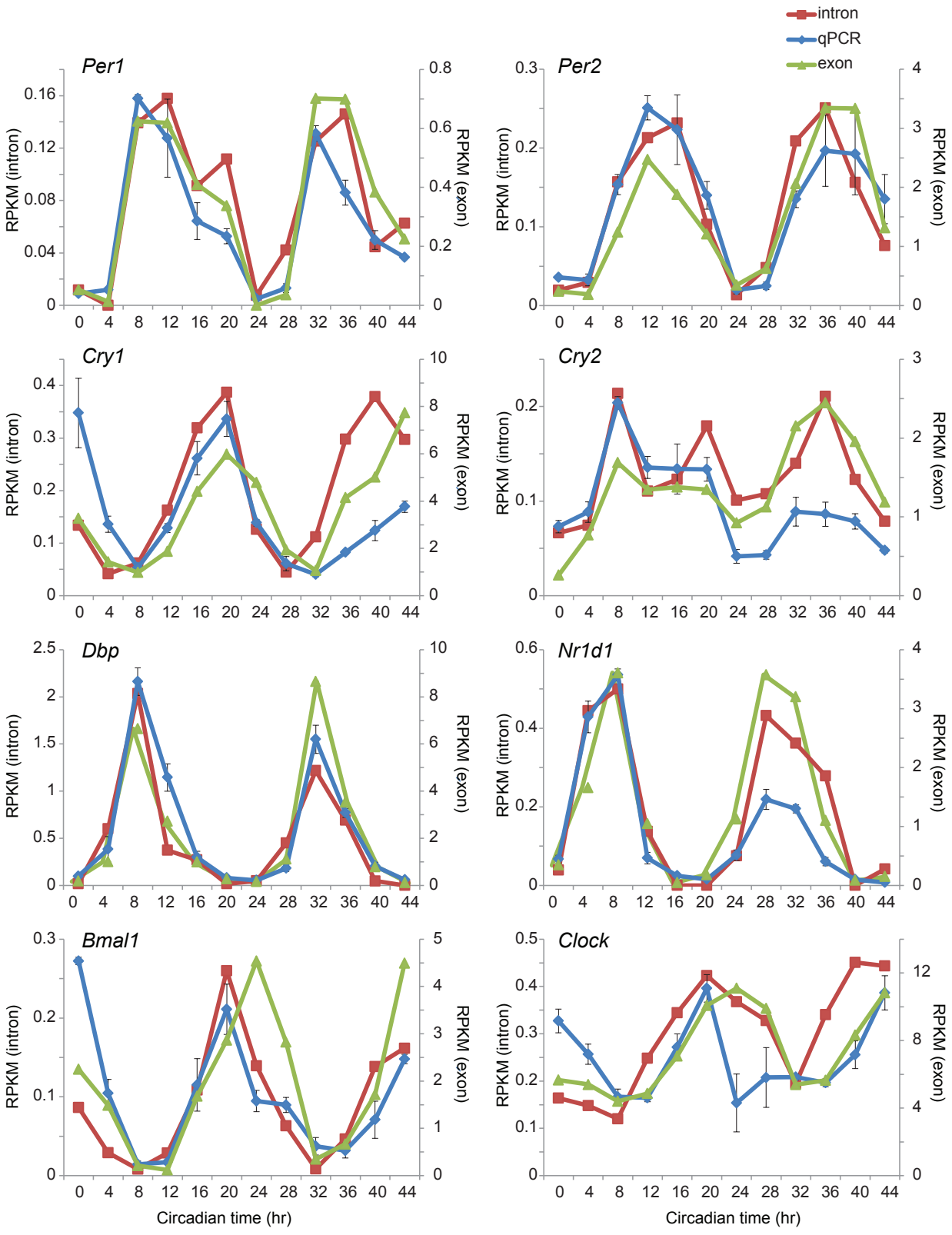
intron
qPCR
exon
Per1
Per2
Cry1
Cry2
Dbp
Nr1d1
Bmal1
Clock
RPKM (intron)
RPKM (exon)
Circadian time (hr)

Fig. S9
A


Scale
chr11:
10 kb
mm9
98629000
98630000
98631000
98632000
98633000
98634000
98635000
98636000
98637000
98638000
98639000
98640000
98641000
98642000
98643000
98644000
98645000
98646000
98647000
98648000
98649000
BMAL1_CT0
BMAL1_CT4
BMAL1_CT8
BMAL1_CT12
BMAL1_CT16
BMAL1_CT20
Bmal1_KO
CLOCK_CT0
CLOCK_CT4
CLOCK_CT8
CLOCK_CT12
CLOCK_CT16
CLOCK_CT20
Clock_KO
NPAS2_CT0
NPAS2_CT4
NPAS2_CT8
NPAS2_CT12
NPAS2_CT16
NPAS2_CT20
PER1_CT0
PER1_CT4
PER1_CT8
PER1_CT12
PER1_CT16
PER1_CT20
Per1/2_KO
PER2_CT0
PER2_CT4
PER2_CT8
PER2_CT12
PER2_CT16
PER2_CT20
Per2_KO
CRY1_CT0
CRY1_CT4
CRY1_CT8
CRY1_CT12
CRY1_CT16
CRY1_CT20
Cry1_KO
CRY2_CT0
CRY2_CT4
CRY2_CT8
CRY2_CT12
CRY2_CT16
CRY2_CT20
Cry1/2_KO
8WG16_CT0
8WG16_CT4
8WG16_CT8
8WG16_CT12
8WG16_CT16
8WG16_CT20
Ser5P_CT0
Ser5P_CT4
Ser5P_CT8
Ser5P_CT12
Ser5P_CT16
Ser5P_CT20
CBP_CT0
CBP_CT4
CBP_CT8
CBP_CT12
CBP_CT16
CBP_CT20
p300_CT0
p300_CT4
p300_CT8
p300_CT12
p300_CT16
p300_CT20
RevErbA_ZT8
RevErbB_ZT8
CT0_RNA_positive
CT0_RNA_negative
CT4_RNA_positive
CT4_RNA_negative
CT8_RNA_positive
CT8_RNA_negative
CT12_RNA_positive
CT12_RNA_negative
CT16_RNA_positive
CT16_RNA_negative
CT20_RNA_positive
CT20_RNA_negative
CT24_RNA_positive
CT24_RNA_negative
CT28_RNA_positive
CT28_RNA_negative
CT32_RNA_positive
CT32_RNA_negative
CT36_RNA_positive
CT36_RNA_negative
CT40_RNA_positive
CT40_RNA_negative
CT44_RNA_positive
CT44_RNA_negative
Thra
Thra
Nr1d1
Mammal Cons

B

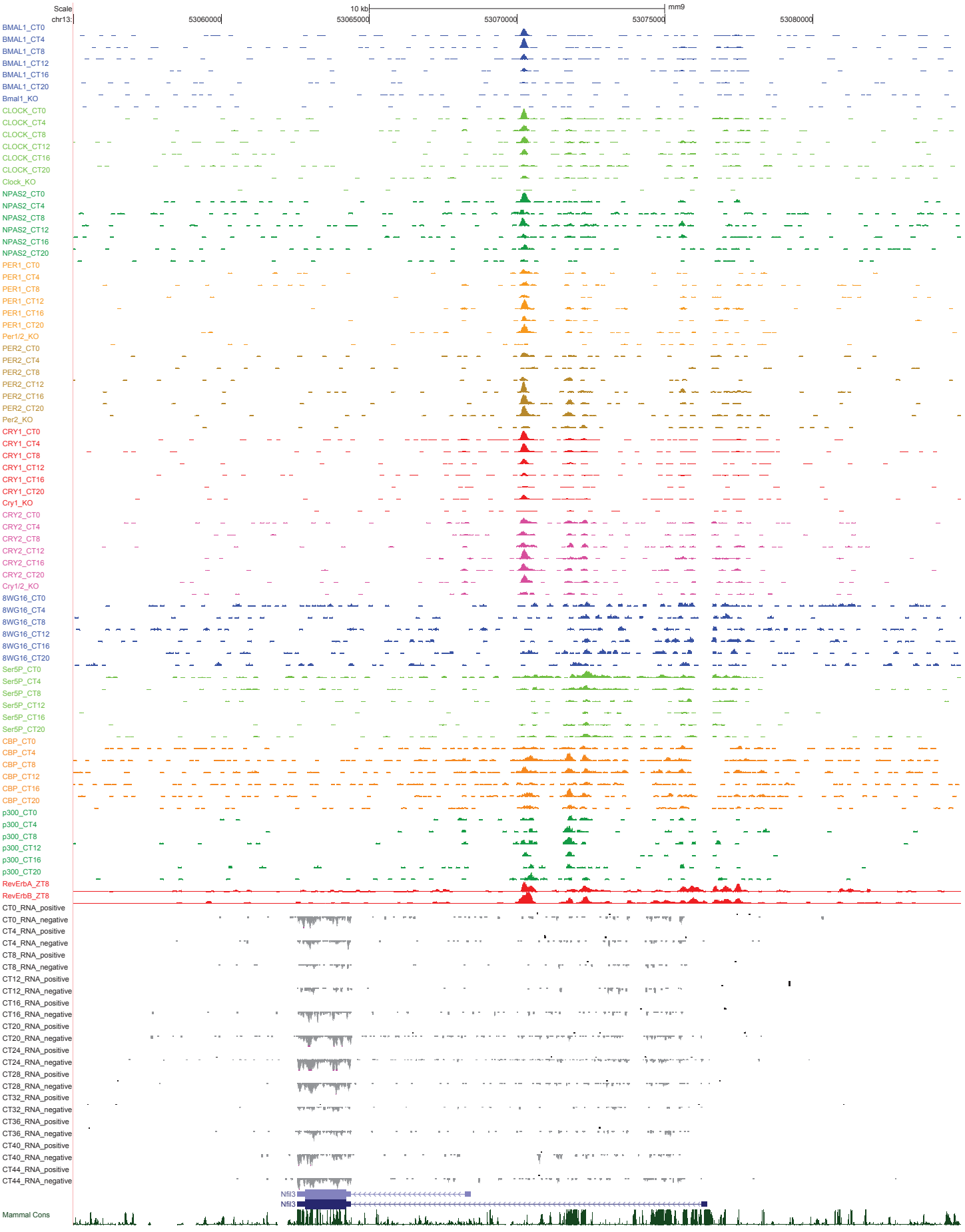
Scale
chr13:
10 kb
mm9
53060000
53065000
53070000
53075000
53080000
BMAL1_CT0
BMAL1_CT4
BMAL1_CT8
BMAL1_CT12
BMAL1_CT16
BMAL1_CT20
Bmal1_KO
CLOCK_CT0
CLOCK_CT4
CLOCK_CT8
CLOCK_CT12
CLOCK_CT16
CLOCK_CT20
Clock_KO
NPAS2_CT0
NPAS2_CT4
NPAS2_CT8
NPAS2_CT12
NPAS2_CT16
NPAS2_CT20
PER1_CT0
PER1_CT4
PER1_CT8
PER1_CT12
PER1_CT16
PER1_CT20
Per1/2_KO
PER2_CT0
PER2_CT4
PER2_CT8
PER2_CT12
PER2_CT16
PER2_CT20
Per2_KO
CRY1_CT0
CRY1_CT4
CRY1_CT8
CRY1_CT12
CRY1_CT16
CRY1_CT20
Cry1_KO
CRY2_CT0
CRY2_CT4
CRY2_CT8
CRY2_CT12
CRY2_CT16
CRY2_CT20
Cry1/2_KO
8WG16_CT0
8WG16_CT4
8WG16_CT8
8WG16_CT12
8WG16_CT16
8WG16_CT20
Ser5P_CT0
Ser5P_CT4
Ser5P_CT8
Ser5P_CT12
Ser5P_CT16
Ser5P_CT20
CBP_CT0
CBP_CT4
CBP_CT8
CBP_CT12
CBP_CT16
CBP_CT20
p300_CT0
p300_CT4
p300_CT8
p300_CT12
p300_CT16
p300_CT20
RevErbA_ZT8
RevErbB_ZT8
CT0_RNA_positive
CT0_RNA_negative
CT4_RNA_positive
CT4_RNA_negative
CT8_RNA_positive
CT8_RNA_negative
CT12_RNA_positive
CT12_RNA_negative
CT16_RNA_positive
CT16_RNA_negative
CT20_RNA_positive
CT20_RNA_negative
CT24_RNA_positive
CT24_RNA_negative
CT28_RNA_positive
CT28_RNA_negative
CT32_RNA_positive
CT32_RNA_negative
CT36_RNA_positive
CT36_RNA_negative
CT40_RNA_positive
CT40_RNA_negative
CT44_RNA_positive
CT44_RNA_negative
Nfil3
Nfil3
Mammal Cons

C

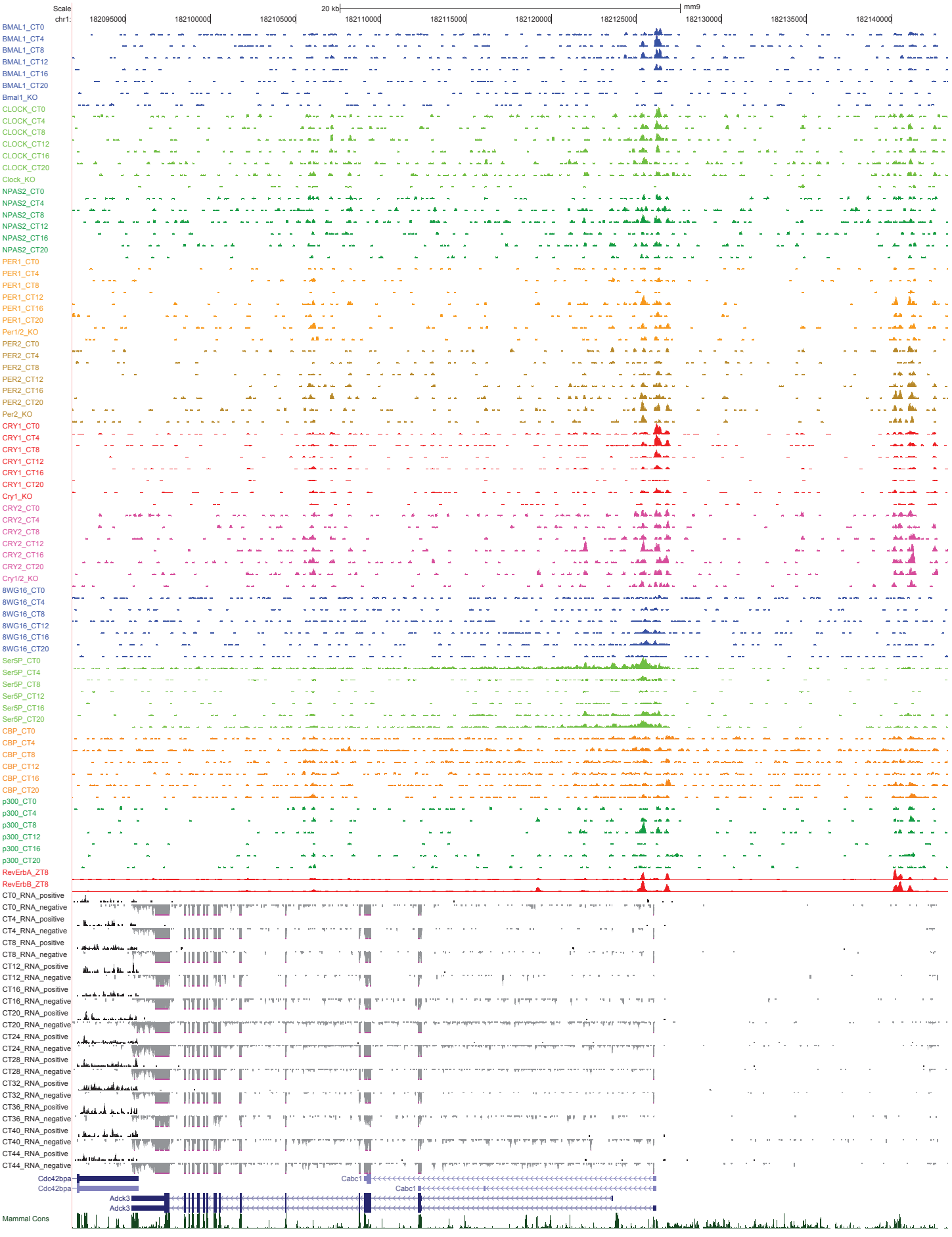
Scale
chr1:
182095000
182100000
182105000
20 kb
182110000
182115000
182120000
182125000
mm9
182130000
182135000
182140000
BMAL1_CT0
BMAL1_CT4
BMAL1_CT8
BMAL1_CT12
BMAL1_CT16
BMAL1_CT20
Bmal1_KO
CLOCK_CT0
CLOCK_CT4
CLOCK_CT8
CLOCK_CT12
CLOCK_CT16
CLOCK_CT20
Clock_KO
NPAS2_CT0
NPAS2_CT4
NPAS2_CT8
NPAS2_CT12
NPAS2_CT16
NPAS2_CT20
PER1_CT0
PER1_CT4
PER1_CT8
PER1_CT12
PER1_CT16
PER1_CT20
Per1/2_KO
PER2_CT0
PER2_CT4
PER2_CT8
PER2_CT12
PER2_CT16
PER2_CT20
Per2_KO
CRY1_CT0
CRY1_CT4
CRY1_CT8
CRY1_CT12
CRY1_CT16
CRY1_CT20
Cry1_KO
CRY2_CT0
CRY2_CT4
CRY2_CT8
CRY2_CT12
CRY2_CT16
CRY2_CT20
Cry1/2_KO
8WG16_CT0
8WG16_CT4
8WG16_CT8
8WG16_CT12
8WG16_CT16
8WG16_CT20
Ser5P_CT0
Ser5P_CT4
Ser5P_CT8
Ser5P_CT12
Ser5P_CT16
Ser5P_CT20
CBP_CT0
CBP_CT4
CBP_CT8
CBP_CT12
CBP_CT16
CBP_CT20
p300_CT0
p300_CT4
p300_CT8
p300_CT12
p300_CT16
p300_CT20
RevErbA_ZT8
RevErbB_ZT8
CT0_RNA_positive
CT0_RNA_negative
CT4_RNA_positive
CT4_RNA_negative
CT8_RNA_positive
CT8_RNA_negative
CT12_RNA_positive
CT12_RNA_negative
CT16_RNA_positive
CT16_RNA_negative
CT20_RNA_positive
CT20_RNA_negative
CT24_RNA_positive
CT24_RNA_negative
CT28_RNA_positive
CT28_RNA_negative
CT32_RNA_positive
CT32_RNA_negative
CT36_RNA_positive
CT36_RNA_negative
CT40_RNA_positive
CT40_RNA_negative
CT44_RNA_positive
CT44_RNA_negative
Cdc42bpa
Cdc42bpa
Cabc1
Cabc1
Adck3
Adck3
Mammal Cons

D


Scale
chr19:
5 kb
mm9
36802000
36803000
36804000
36805000
36806000
36807000
36808000
36809000
36810000
36811000
36812000
36813000
36814000
36815000
BMAL1_CT0
BMAL1_CT4
BMAL1_CT8
BMAL1_CT12
BMAL1_CT16
BMAL1_CT20
Bmal1_KO
CLOCK_CT0
CLOCK_CT4
CLOCK_CT8
CLOCK_CT12
CLOCK_CT16
CLOCK_CT20
Clock_KO
NPAS2_CT0
NPAS2_CT4
NPAS2_CT8
NPAS2_CT12
NPAS2_CT16
NPAS2_CT20
PER1_CT0
PER1_CT4
PER1_CT8
PER1_CT12
PER1_CT16
PER1_CT20
Per1/2_KO
PER2_CT0
PER2_CT4
PER2_CT8
PER2_CT12
PER2_CT16
PER2_CT20
Per2_KO
CRY1_CT0
CRY1_CT4
CRY1_CT8
CRY1_CT12
CRY1_CT16
CRY1_CT20
Cry1_KO
CRY2_CT0
CRY2_CT4
CRY2_CT8
CRY2_CT12
CRY2_CT16
CRY2_CT20
Cry1/2_KO
8WG16_CT0
8WG16_CT4
8WG16_CT8
8WG16_CT12
8WG16_CT16
8WG16_CT20
Ser5P_CT0
Ser5P_CT4
Ser5P_CT8
Ser5P_CT12
Ser5P_CT16
Ser5P_CT20
CBP_CT0
CBP_CT4
CBP_CT8
CBP_CT12
CBP_CT16
CBP_CT20
p300_CT0
p300_CT4
p300_CT8
p300_CT12
p300_CT16
p300_CT20
RevErbA_ZT8
RevErbB_ZT8
CT0_RNA_positive
CT0_RNA_negative
CT4_RNA_positive
CT4_RNA_negative
CT8_RNA_positive
CT8_RNA_negative
CT12_RNA_positive
CT12_RNA_negative
CT16_RNA_positive
CT16_RNA_negative
CT20_RNA_positive
CT20_RNA_negative
CT24_RNA_positive
CT24_RNA_negative
CT28_RNA_positive
CT28_RNA_negative
CT32_RNA_positive
CT32_RNA_negative
CT36_RNA_positive
CT36_RNA_negative
CT40_RNA_positive
CT40_RNA_negative
CT44_RNA_positive
CT44_RNA_negative
Ppp1r3c
Mammal Cons

Fig. S10

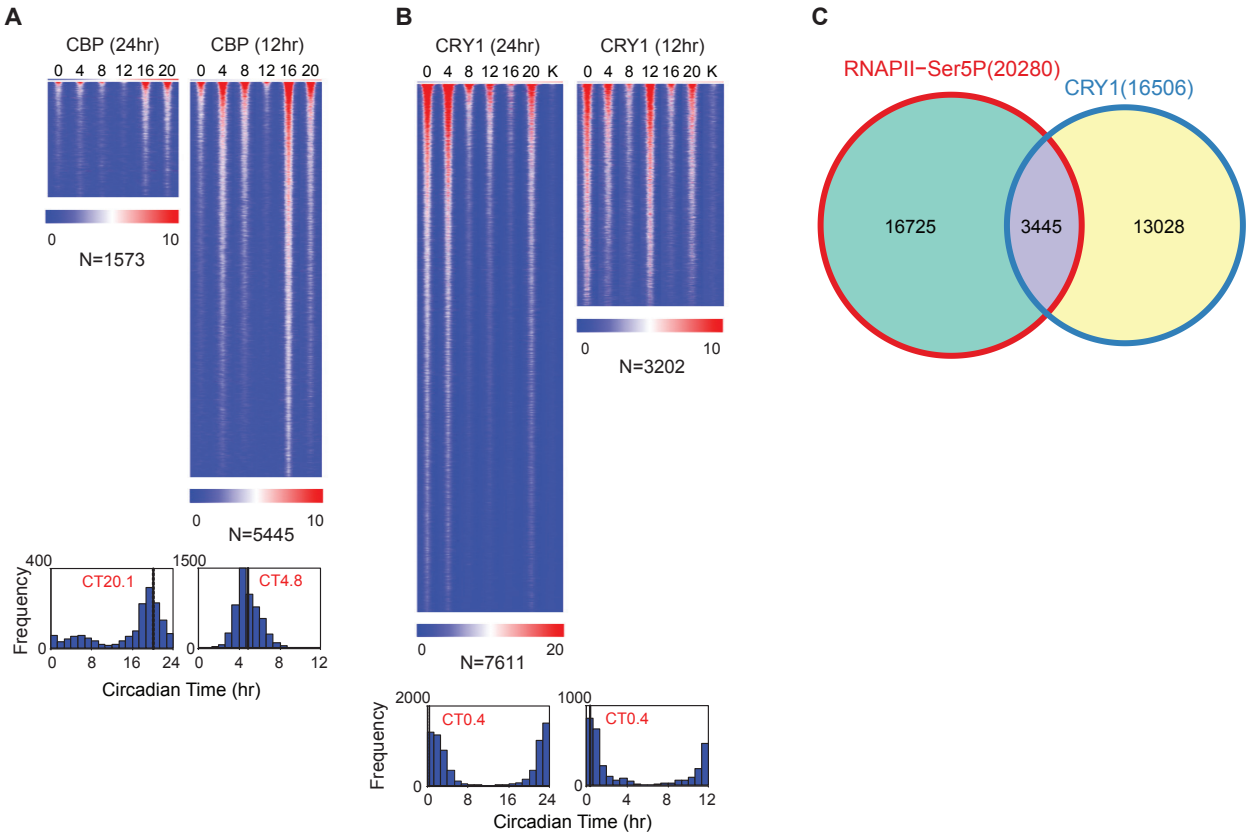
A
CBP (24hr)
CBP (12hr)
0 4 8 12 16 20
0
10
N=1573
N=5445
400
1500
CT20.1
CT4.8
Frequency
0 8 16 24
0 4 8 12
Circadian Time (hr)
B
CRY1 (24hr)
CRY1 (12hr)
0 4 8 12 16 20 K
0
20
N=7611
N=3202
2000
1000
CT0.4
CT0.4
Frequency
0 8 16 24
0 4 8 12
Circadian Time (hr)
C
RNAPII−Ser5P(20280)
CRY1(16506)
16725
3445
13028

Fig. S11

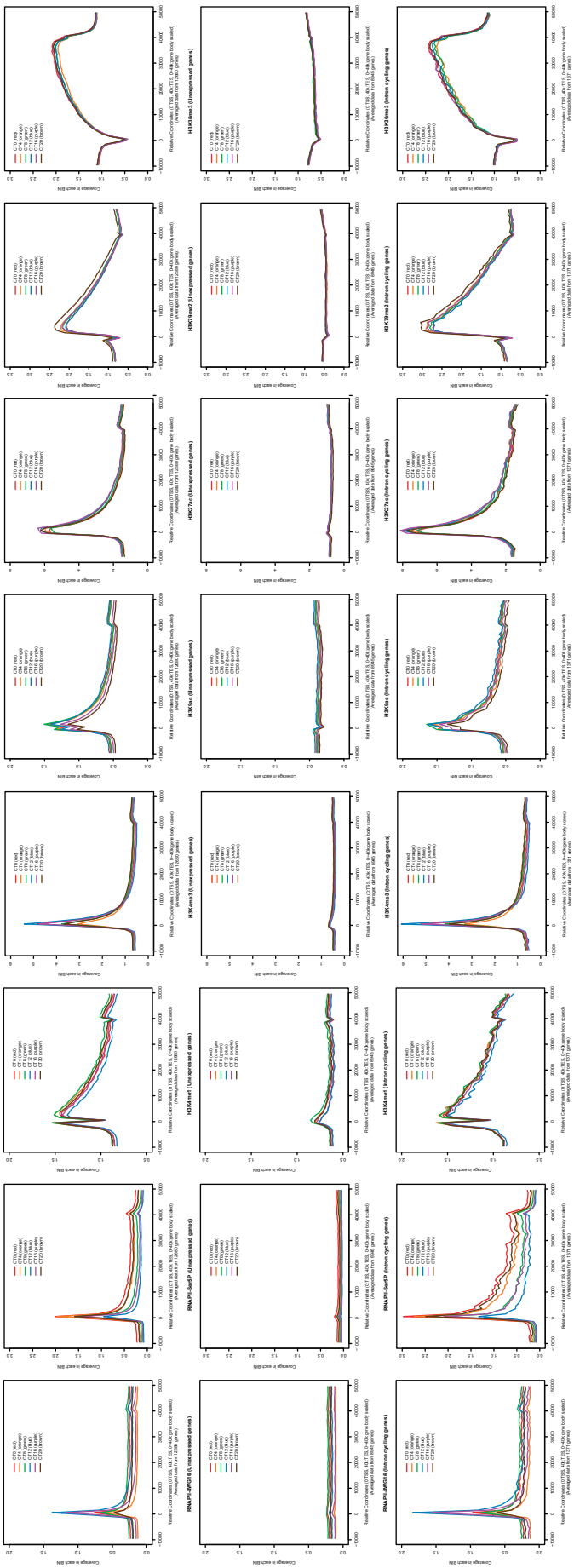

Fig. S12

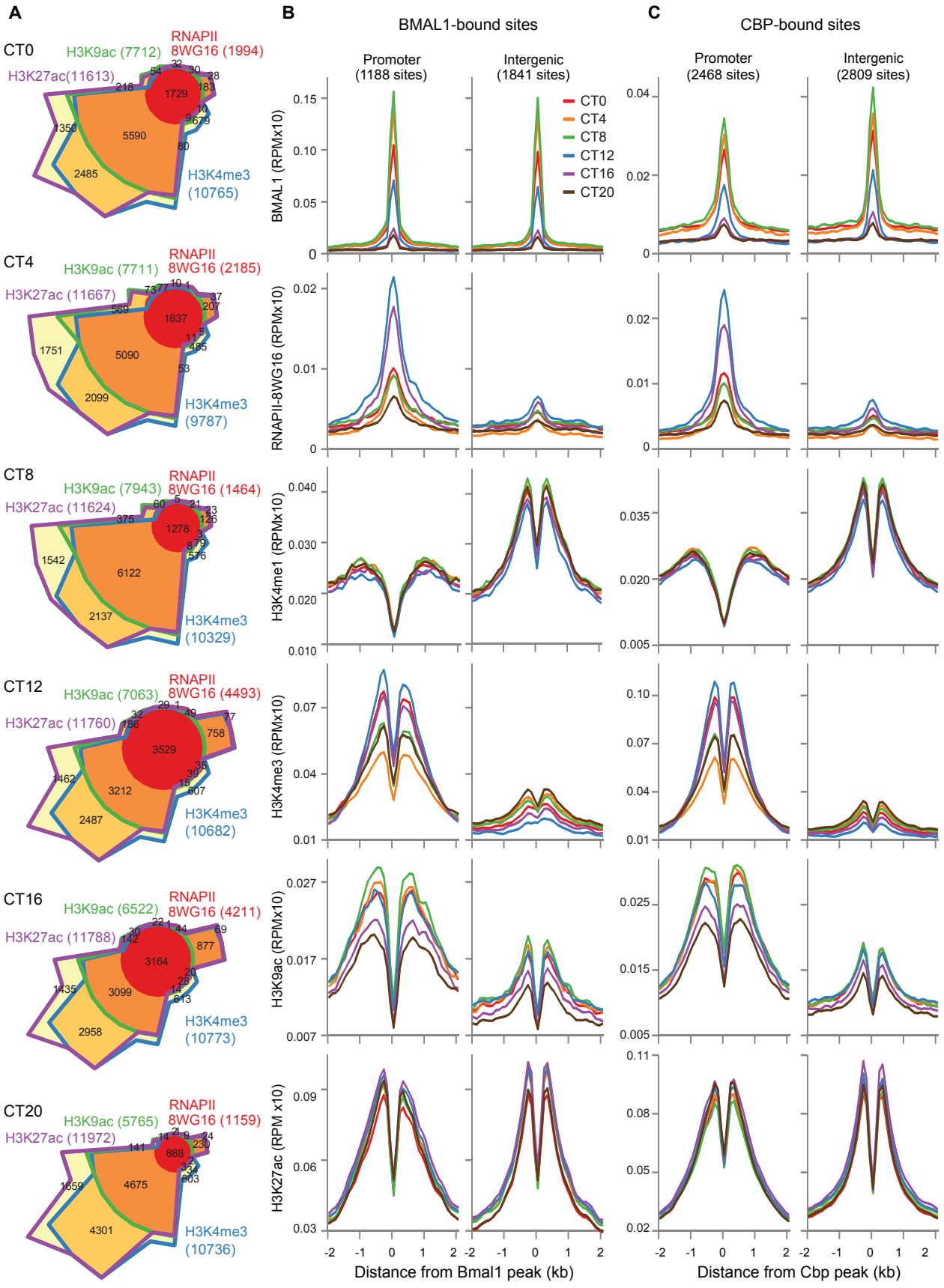
A
B
C
BMAL1-bound sites
CBP-bound sites
Promoter (1188 sites)
Intergenic (1841 sites)
Promoter (2468 sites)
Intergenic (2809 sites)
CT0
CT4
CT8
CT12
CT16
CT20
H3K9ac (7712)
RNAPII 8WG16 (1994)
H3K27ac(11613)
H3K4me3 (10765)
H3K9ac (7711)
RNAPII 8WG16 (2185)
H3K27ac (11667)
H3K4me3 (9787)
H3K9ac (7943)
RNAPII 8WG16 (1464)
H3K27ac (11624)
H3K4me3 (10329)
H3K9ac (7063)
RNAPII 8WG16 (4493)
H3K27ac (11760)
H3K4me3 (10682)
H3K9ac (6522)
RNAPII 8WG16 (4211)
H3K27ac (11788)
H3K4me3 (10773)
H3K9ac (5765)
RNAPII 8WG16 (1159)
H3K27ac (11972)
H3K4me3 (10736)
BMAL1 (RPMx10)
RNAPII-8WG16 (RPMx10)
H3K4me1 (RPMx10)
H3K4me3 (RPMx10)
H3K9ac (RPMx10)
H3K27ac (RPM x10)
Distance from Bmal1 peak (kb)
Distance from Cbp peak (kb)

Fig. S13

A

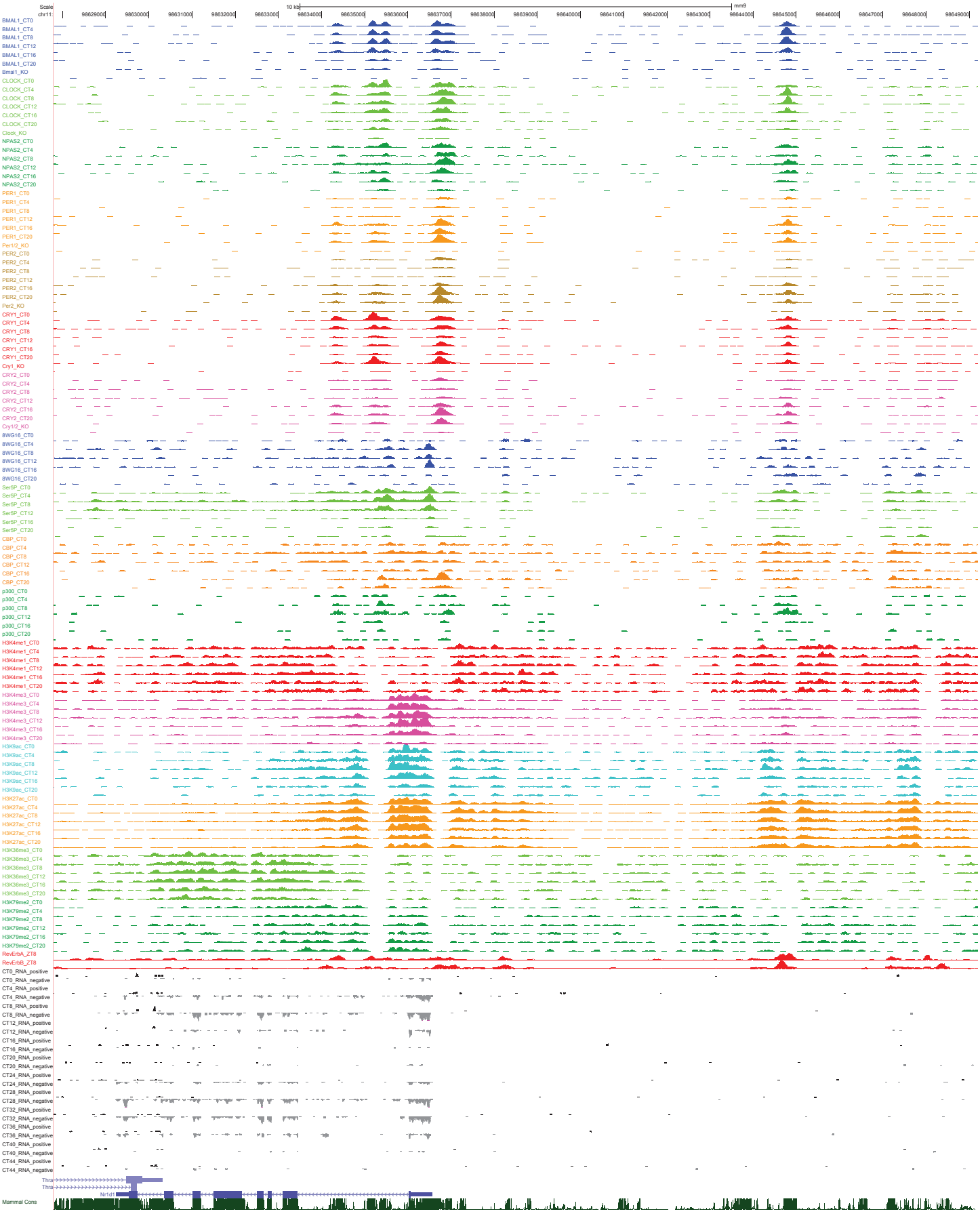
Scale
chr11:
10 kb
mm9
98629000
98630000
98631000
98632000
98633000
98634000
98635000
98636000
98637000
98638000
98639000
98640000
98641000
98642000
98643000
98644000
98645000
98646000
98647000
98648000
98649000
BMAL1_CT0
BMAL1_CT4
BMAL1_CT8
BMAL1_CT12
BMAL1_CT16
BMAL1_CT20
Bmal1_KO
CLOCK_CT0
CLOCK_CT4
CLOCK_CT8
CLOCK_CT12
CLOCK_CT16
CLOCK_CT20
Clock_KO
NPAS2_CT0
NPAS2_CT4
NPAS2_CT8
NPAS2_CT12
NPAS2_CT16
NPAS2_CT20
PER1_CT0
PER1_CT4
PER1_CT8
PER1_CT12
PER1_CT16
PER1_CT20
Per1/2_KO
PER2_CT0
PER2_CT4
PER2_CT8
PER2_CT12
PER2_CT16
PER2_CT20
Per2_KO
CRY1_CT0
CRY1_CT4
CRY1_CT8
CRY1_CT12
CRY1_CT16
CRY1_CT20
Cry1_KO
CRY2_CT0
CRY2_CT4
CRY2_CT8
CRY2_CT12
CRY2_CT16
CRY2_CT20
Cry1/2_KO
BWG16_CT0
BWG16_CT4
BWG16_CT8
BWG16_CT12
BWG16_CT16
BWG16_CT20
Ser5P_CT0
Ser5P_CT4
Ser5P_CT8
Ser5P_CT12
Ser5P_CT16
Ser5P_CT20
CBP_CT0
CBP_CT4
CBP_CT8
CBP_CT12
CBP_CT16
CBP_CT20
p300_CT0
p300_CT4
p300_CT8
p300_CT12
p300_CT16
p300_CT20
H3K4me1_CT0
H3K4me1_CT4
H3K4me1_CT8
H3K4me1_CT12
H3K4me1_CT16
H3K4me1_CT20
H3K4me3_CT0
H3K4me3_CT4
H3K4me3_CT8
H3K4me3_CT12
H3K4me3_CT16
H3K4me3_CT20
H3K9ac_CT0
H3K9ac_CT4
H3K9ac_CT8
H3K9ac_CT12
H3K9ac_CT16
H3K9ac_CT20
H3K27ac_CT0
H3K27ac_CT4
H3K27ac_CT8
H3K27ac_CT12
H3K27ac_CT16
H3K27ac_CT20
H3K36me3_CT0
H3K36me3_CT4
H3K36me3_CT8
H3K36me3_CT12
H3K36me3_CT16
H3K36me3_CT20
H3K79me2_CT0
H3K79me2_CT4
H3K79me2_CT8
H3K79me2_CT12
H3K79me2_CT16
H3K79me2_CT20
RevErbA_ZT8
RevErbB_ZT8
CT0_RNA_positive
CT0_RNA_negative
CT4_RNA_positive
CT4_RNA_negative
CT8_RNA_positive
CT8_RNA_negative
CT12_RNA_positive
CT12_RNA_negative
CT16_RNA_positive
CT16_RNA_negative
CT20_RNA_positive
CT20_RNA_negative
CT24_RNA_positive
CT24_RNA_negative
CT28_RNA_positive
CT28_RNA_negative
CT32_RNA_positive
CT32_RNA_negative
CT36_RNA_positive
CT36_RNA_negative
CT40_RNA_positive
CT40_RNA_negative
CT44_RNA_positive
CT44_RNA_negative
Thra
Thra
Nr1d1
Mammal Cons

B

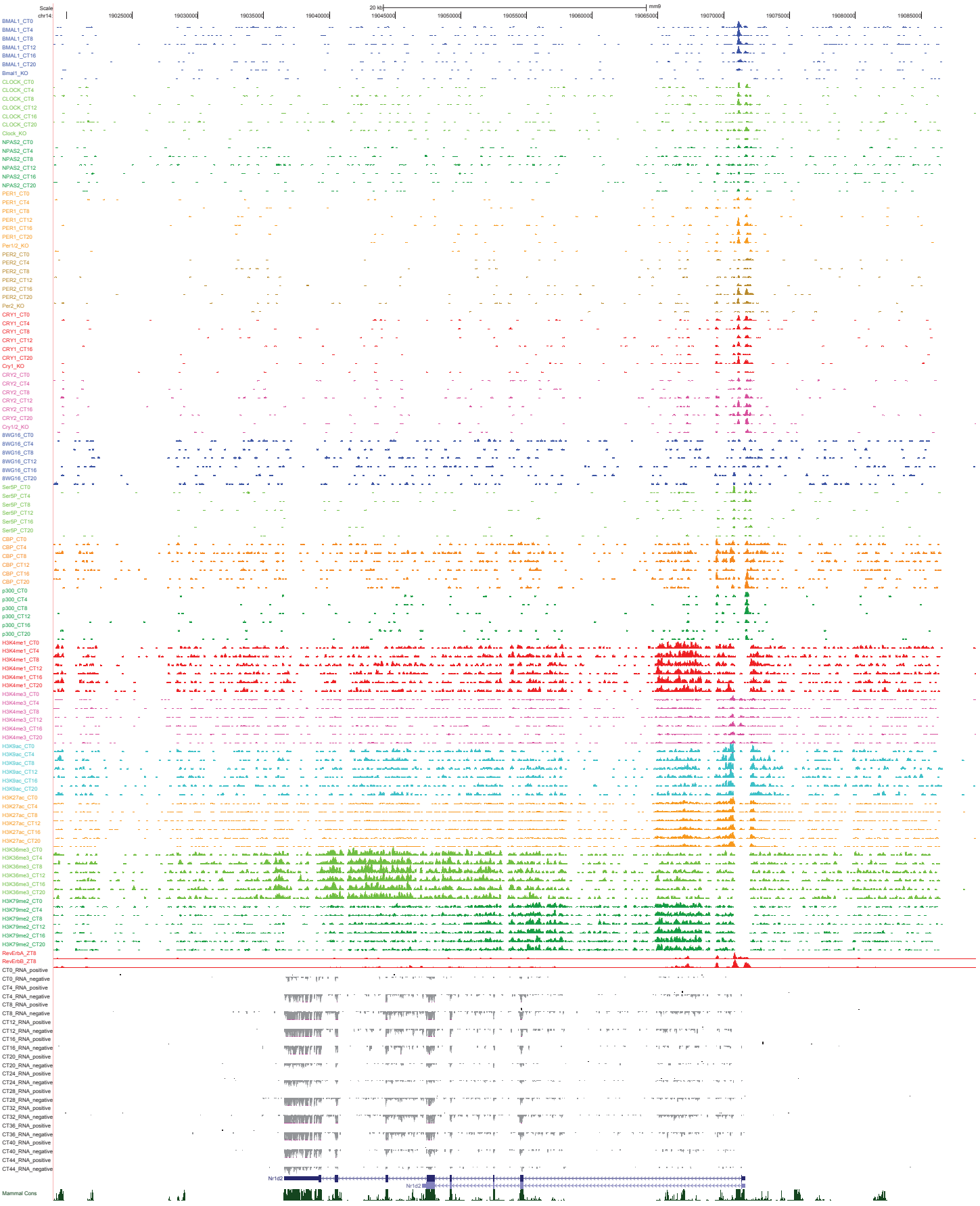
Scale
chr14:
20 kb
mm9
19025000
19030000
19035000
19040000
19045000
19050000
19055000
19060000
19065000
19070000
19075000
19080000
19085000
BMAL1_CT0
BMAL1_CT4
BMAL1_CT8
BMAL1_CT12
BMAL1_CT16
BMAL1_CT20
Bmal1_KO
CLOCK_CT0
CLOCK_CT4
CLOCK_CT8
CLOCK_CT12
CLOCK_CT16
CLOCK_CT20
Clock_KO
NPAS2_CT0
NPAS2_CT4
NPAS2_CT8
NPAS2_CT12
NPAS2_CT16
NPAS2_CT20
PER1_CT0
PER1_CT4
PER1_CT8
PER1_CT12
PER1_CT16
PER1_CT20
Per1/2_KO
PER2_CT0
PER2_CT4
PER2_CT8
PER2_CT12
PER2_CT16
PER2_CT20
Per2_KO
CRY1_CT0
CRY1_CT4
CRY1_CT8
CRY1_CT12
CRY1_CT16
CRY1_CT20
Cry1_KO
CRY2_CT0
CRY2_CT4
CRY2_CT8
CRY2_CT12
CRY2_CT16
CRY2_CT20
Cry1/2_KO
8WG16_CT0
8WG16_CT4
8WG16_CT8
8WG16_CT12
8WG16_CT16
8WG16_CT20
Ser5P_CT0
Ser5P_CT4
Ser5P_CT8
Ser5P_CT12
Ser5P_CT16
Ser5P_CT20
CBP_CT0
CBP_CT4
CBP_CT8
CBP_CT12
CBP_CT16
CBP_CT20
p300_CT0
p300_CT4
p300_CT8
p300_CT12
p300_CT16
p300_CT20
H3K4me1_CT0
H3K4me1_CT4
H3K4me1_CT8
H3K4me1_CT12
H3K4me1_CT16
H3K4me1_CT20
H3K4me3_CT0
H3K4me3_CT4
H3K4me3_CT8
H3K4me3_CT12
H3K4me3_CT16
H3K4me3_CT20
H3K9ac_CT0
H3K9ac_CT4
H3K9ac_CT8
H3K9ac_CT12
H3K9ac_CT16
H3K9ac_CT20
H3K27ac_CT0
H3K27ac_CT4
H3K27ac_CT8
H3K27ac_CT12
H3K27ac_CT16
H3K27ac_CT20
H3K36me3_CT0
H3K36me3_CT4
H3K36me3_CT8
H3K36me3_CT12
H3K36me3_CT16
H3K36me3_CT20
H3K79me2_CT0
H3K79me2_CT4
H3K79me2_CT8
H3K79me2_CT12
H3K79me2_CT16
H3K79me2_CT20
RevErbA_ZT8
RevErbB_ZT8
CT0_RNA_positive
CT0_RNA_negative
CT4_RNA_positive
CT4_RNA_negative
CT8_RNA_positive
CT8_RNA_negative
CT12_RNA_positive
CT12_RNA_negative
CT16_RNA_positive
CT16_RNA_negative
CT20_RNA_positive
CT20_RNA_negative
CT24_RNA_positive
CT24_RNA_negative
CT28_RNA_positive
CT28_RNA_negative
CT32_RNA_positive
CT32_RNA_negative
CT36_RNA_positive
CT36_RNA_negative
CT40_RNA_positive
CT40_RNA_negative
CT44_RNA_positive
CT44_RNA_negative
Nr1d2
Nr1d2
Mammal Cons

C

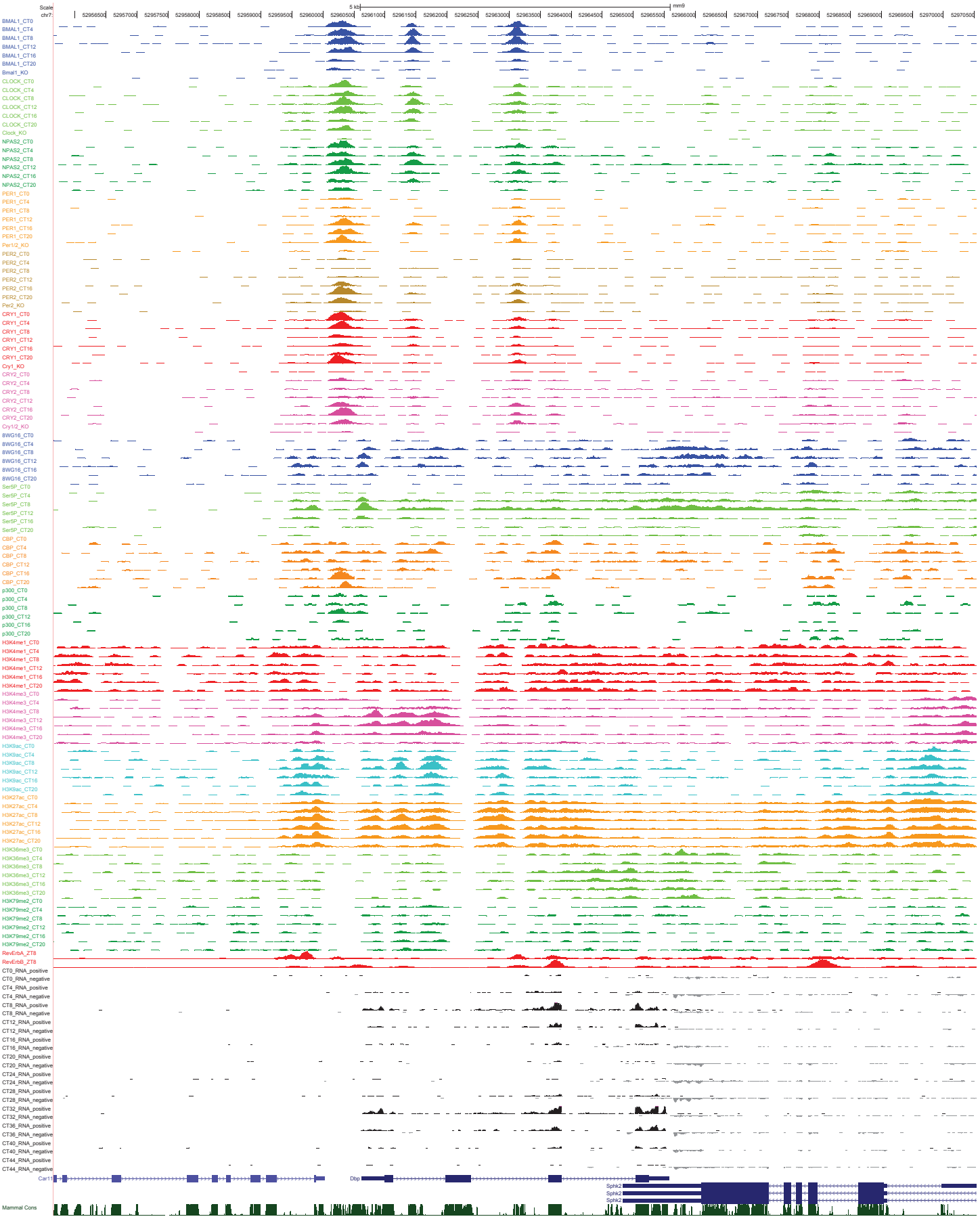
Scale
chr7:
5 kb
mm9
BMAL1_CT0
BMAL1_CT4
BMAL1_CT8
BMAL1_CT12
BMAL1_CT16
BMAL1_CT20
Bmal1_KO
CLOCK_CT0
CLOCK_CT4
CLOCK_CT8
CLOCK_CT12
CLOCK_CT16
CLOCK_CT20
Clock_KO
NPAS2_CT0
NPAS2_CT4
NPAS2_CT8
NPAS2_CT12
NPAS2_CT16
NPAS2_CT20
PER1_CT0
PER1_CT4
PER1_CT8
PER1_CT12
PER1_CT16
PER1_CT20
Per1/2_KO
PER2_CT0
PER2_CT4
PER2_CT8
PER2_CT12
PER2_CT16
PER2_CT20
Per2_KO
CRY1_CT0
CRY1_CT4
CRY1_CT8
CRY1_CT12
CRY1_CT16
CRY1_CT20
Cry1_KO
CRY2_CT0
CRY2_CT4
CRY2_CT8
CRY2_CT12
CRY2_CT16
CRY2_CT20
Cry1/2_KO
8WG16_CT0
8WG16_CT4
8WG16_CT8
8WG16_CT12
8WG16_CT16
8WG16_CT20
Ser5P_CT0
Ser5P_CT4
Ser5P_CT8
Ser5P_CT12
Ser5P_CT16
Ser5P_CT20
CBP_CT0
CBP_CT4
CBP_CT8
CBP_CT12
CBP_CT16
CBP_CT20
p300_CT0
p300_CT4
p300_CT8
p300_CT12
p300_CT16
p300_CT20
H3K4me1_CT0
H3K4me1_CT4
H3K4me1_CT8
H3K4me1_CT12
H3K4me1_CT16
H3K4me1_CT20
H3K4me3_CT0
H3K4me3_CT4
H3K4me3_CT8
H3K4me3_CT12
H3K4me3_CT16
H3K4me3_CT20
H3K9ac_CT0
H3K9ac_CT4
H3K9ac_CT8
H3K9ac_CT12
H3K9ac_CT16
H3K9ac_CT20
H3K27ac_CT0
H3K27ac_CT4
H3K27ac_CT8
H3K27ac_CT12
H3K27ac_CT16
H3K27ac_CT20
H3K36me3_CT0
H3K36me3_CT4
H3K36me3_CT8
H3K36me3_CT12
H3K36me3_CT16
H3K36me3_CT20
H3K79me2_CT0
H3K79me2_CT4
H3K79me2_CT8
H3K79me2_CT12
H3K79me2_CT16
H3K79me2_CT20
RevErbA_ZT8
RevErbB_ZT8
CT0_RNA_positive
CT0_RNA_negative
CT4_RNA_positive
CT4_RNA_negative
CT8_RNA_positive
CT8_RNA_negative
CT12_RNA_positive
CT12_RNA_negative
CT16_RNA_positive
CT16_RNA_negative
CT20_RNA_positive
CT20_RNA_negative
CT24_RNA_positive
CT24_RNA_negative
CT28_RNA_positive
CT28_RNA_negative
CT32_RNA_positive
CT32_RNA_negative
CT36_RNA_positive
CT36_RNA_negative
CT40_RNA_positive
CT40_RNA_negative
CT44_RNA_positive
CT44_RNA_negative
Car11
Dbp
Sphk2
Sphk2
Sphk2
Mammal Cons

D

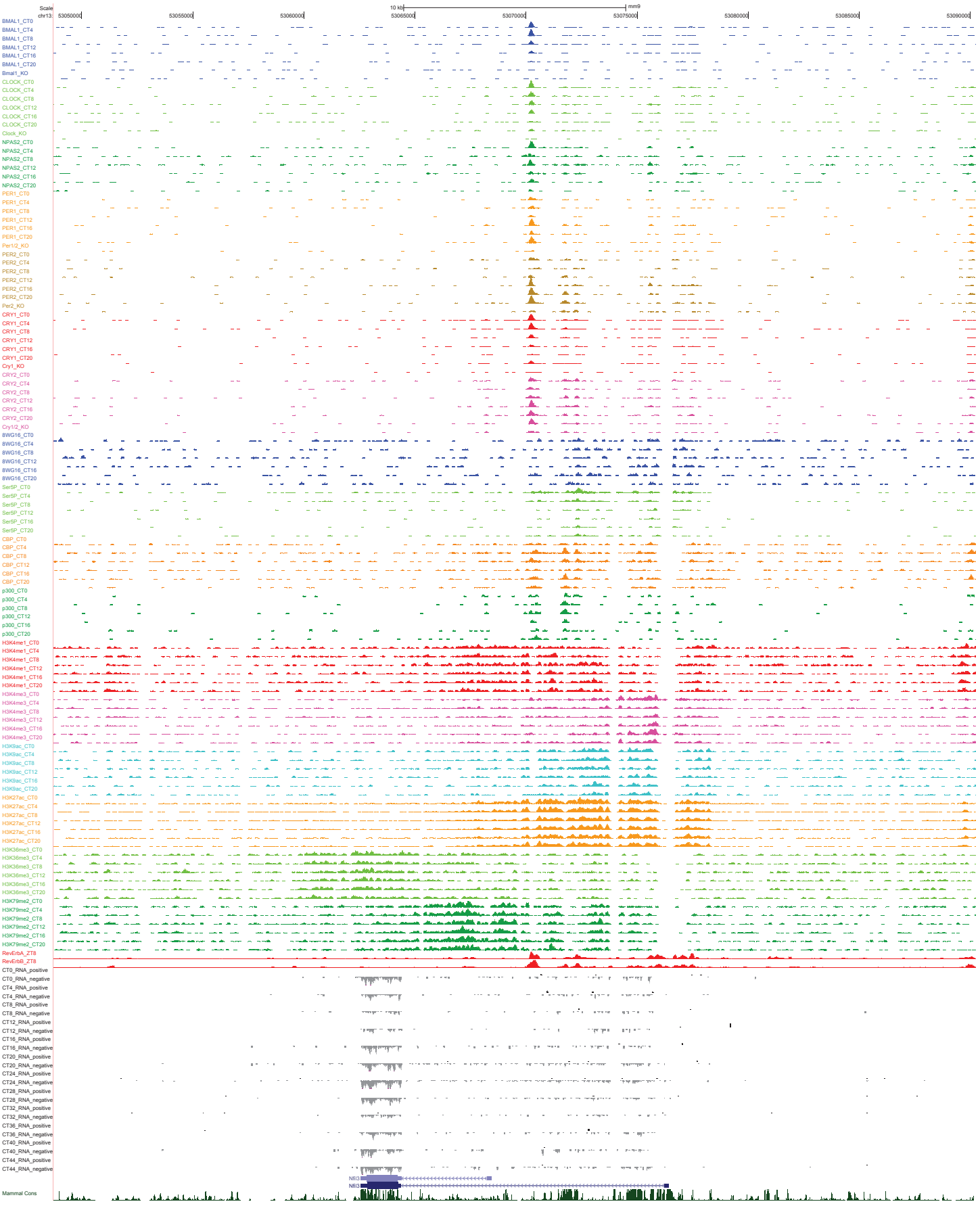
Scale
chr13:
53050000
53055000
53060000
10 kb
53065000
53070000
53075000
mm9
53080000
53085000
53090000
BMAL1_CT0
BMAL1_CT4
BMAL1_CT8
BMAL1_CT12
BMAL1_CT16
BMAL1_CT20
Bmal1_KO
CLOCK_CT0
CLOCK_CT4
CLOCK_CT8
CLOCK_CT12
CLOCK_CT16
CLOCK_CT20
Clock_KO
NPAS2_CT0
NPAS2_CT4
NPAS2_CT8
NPAS2_CT12
NPAS2_CT16
NPAS2_CT20
PER1_CT0
PER1_CT4
PER1_CT8
PER1_CT12
PER1_CT16
PER1_CT20
Per1/2_KO
PER2_CT0
PER2_CT4
PER2_CT8
PER2_CT12
PER2_CT16
PER2_CT20
Per2_KO
CRY1_CT0
CRY1_CT4
CRY1_CT8
CRY1_CT12
CRY1_CT16
CRY1_CT20
Cry1_KO
CRY2_CT0
CRY2_CT4
CRY2_CT8
CRY2_CT12
CRY2_CT16
CRY2_CT20
Cry1/2_KO
BWG16_CT0
BWG16_CT4
BWG16_CT8
BWG16_CT12
BWG16_CT16
BWG16_CT20
Ser5P_CT0
Ser5P_CT4
Ser5P_CT8
Ser5P_CT12
Ser5P_CT16
Ser5P_CT20
CBP_CT0
CBP_CT4
CBP_CT8
CBP_CT12
CBP_CT16
CBP_CT20
p300_CT0
p300_CT4
p300_CT8
p300_CT12
p300_CT16
p300_CT20
H3K4me1_CT0
H3K4me1_CT4
H3K4me1_CT8
H3K4me1_CT12
H3K4me1_CT16
H3K4me1_CT20
H3K4me3_CT0
H3K4me3_CT4
H3K4me3_CT8
H3K4me3_CT12
H3K4me3_CT16
H3K4me3_CT20
H3K9ac_CT0
H3K9ac_CT4
H3K9ac_CT8
H3K9ac_CT12
H3K9ac_CT16
H3K9ac_CT20
H3K27ac_CT0
H3K27ac_CT4
H3K27ac_CT8
H3K27ac_CT12
H3K27ac_CT16
H3K27ac_CT20
H3K36me3_CT0
H3K36me3_CT4
H3K36me3_CT8
H3K36me3_CT12
H3K36me3_CT16
H3K36me3_CT20
H3K79me2_CT0
H3K79me2_CT4
H3K79me2_CT8
H3K79me2_CT12
H3K79me2_CT16
H3K79me2_CT20
RevErbA_ZT8
RevErbB_ZT8
CT0_RNA_positive
CT0_RNA_negative
CT4_RNA_positive
CT4_RNA_negative
CT8_RNA_positive
CT8_RNA_negative
CT12_RNA_positive
CT12_RNA_negative
CT16_RNA_positive
CT16_RNA_negative
CT20_RNA_positive
CT20_RNA_negative
CT24_RNA_positive
CT24_RNA_negative
CT28_RNA_positive
CT28_RNA_negative
CT32_RNA_positive
CT32_RNA_negative
CT36_RNA_positive
CT36_RNA_negative
CT40_RNA_positive
CT40_RNA_negative
CT44_RNA_positive
CT44_RNA_negative
NBl3
NBl3
Mammal Cons

E

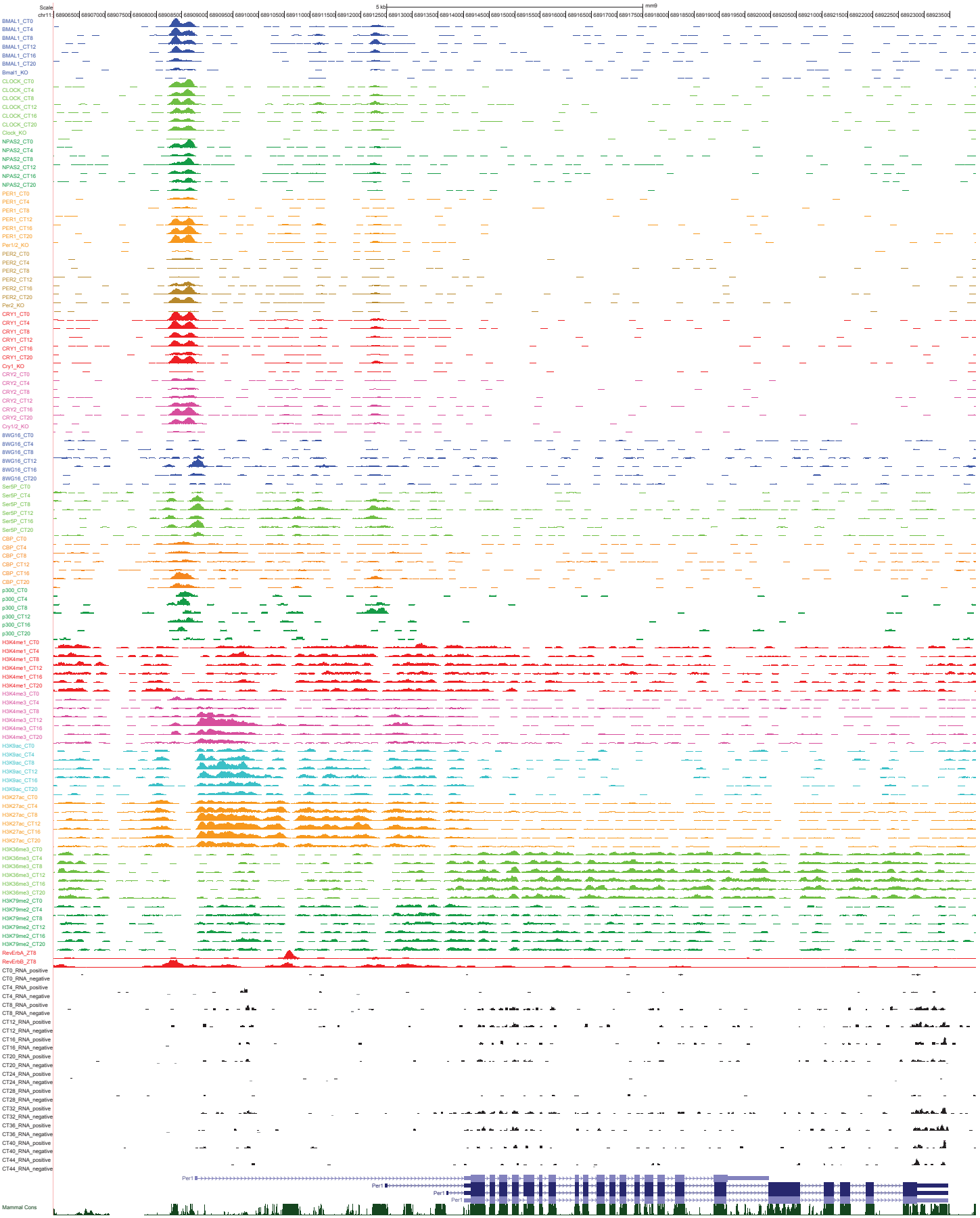
Scale
chr11
5 kb
mm9
BMAL1_CT0
BMAL1_CT4
BMAL1_CT8
BMAL1_CT12
BMAL1_CT16
BMAL1_CT20
Bmal1_KO
CLOCK_CT0
CLOCK_CT4
CLOCK_CT8
CLOCK_CT12
CLOCK_CT16
CLOCK_CT20
Clock_KO
NPAS2_CT0
NPAS2_CT4
NPAS2_CT8
NPAS2_CT12
NPAS2_CT16
NPAS2_CT20
PER1_CT0
PER1_CT4
PER1_CT8
PER1_CT12
PER1_CT16
PER1_CT20
Per1/2_KO
PER2_CT0
PER2_CT4
PER2_CT8
PER2_CT12
PER2_CT16
PER2_CT20
Per2_KO
CRY1_CT0
CRY1_CT4
CRY1_CT8
CRY1_CT12
CRY1_CT16
CRY1_CT20
Cry1_KO
CRY2_CT0
CRY2_CT4
CRY2_CT8
CRY2_CT12
CRY2_CT16
CRY2_CT20
Cry1/2_KO
BWG16_CT0
BWG16_CT4
BWG16_CT8
BWG16_CT12
BWG16_CT16
BWG16_CT20
Ser5P_CT0
Ser5P_CT4
Ser5P_CT8
Ser5P_CT12
Ser5P_CT16
Ser5P_CT20
CBP_CT0
CBP_CT4
CBP_CT8
CBP_CT12
CBP_CT16
CBP_CT20
p300_CT0
p300_CT4
p300_CT8
p300_CT12
p300_CT16
p300_CT20
H3K4me1_CT0
H3K4me1_CT4
H3K4me1_CT8
H3K4me1_CT12
H3K4me1_CT16
H3K4me1_CT20
H3K4me3_CT0
H3K4me3_CT4
H3K4me3_CT8
H3K4me3_CT12
H3K4me3_CT16
H3K4me3_CT20
H3K9ac_CT0
H3K9ac_CT4
H3K9ac_CT8
H3K9ac_CT12
H3K9ac_CT16
H3K9ac_CT20
H3K27ac_CT0
H3K27ac_CT4
H3K27ac_CT8
H3K27ac_CT12
H3K27ac_CT16
H3K27ac_CT20
H3K36me3_CT0
H3K36me3_CT4
H3K36me3_CT8
H3K36me3_CT12
H3K36me3_CT16
H3K36me3_CT20
H3K79me2_CT0
H3K79me2_CT4
H3K79me2_CT8
H3K79me2_CT12
H3K79me2_CT16
H3K79me2_CT20
RevErbA_ZT8
RevErbB_ZT8
CT0_RNA_positive
CT0_RNA_negative
CT4_RNA_positive
CT4_RNA_negative
CT8_RNA_positive
CT8_RNA_negative
CT12_RNA_positive
CT12_RNA_negative
CT16_RNA_positive
CT16_RNA_negative
CT20_RNA_positive
CT20_RNA_negative
CT24_RNA_positive
CT24_RNA_negative
CT28_RNA_positive
CT28_RNA_negative
CT32_RNA_positive
CT32_RNA_negative
CT36_RNA_positive
CT36_RNA_negative
CT40_RNA_positive
CT40_RNA_negative
CT44_RNA_positive
CT44_RNA_negative
Per1
Per1
Per1
Per1
Mammal Cons

F

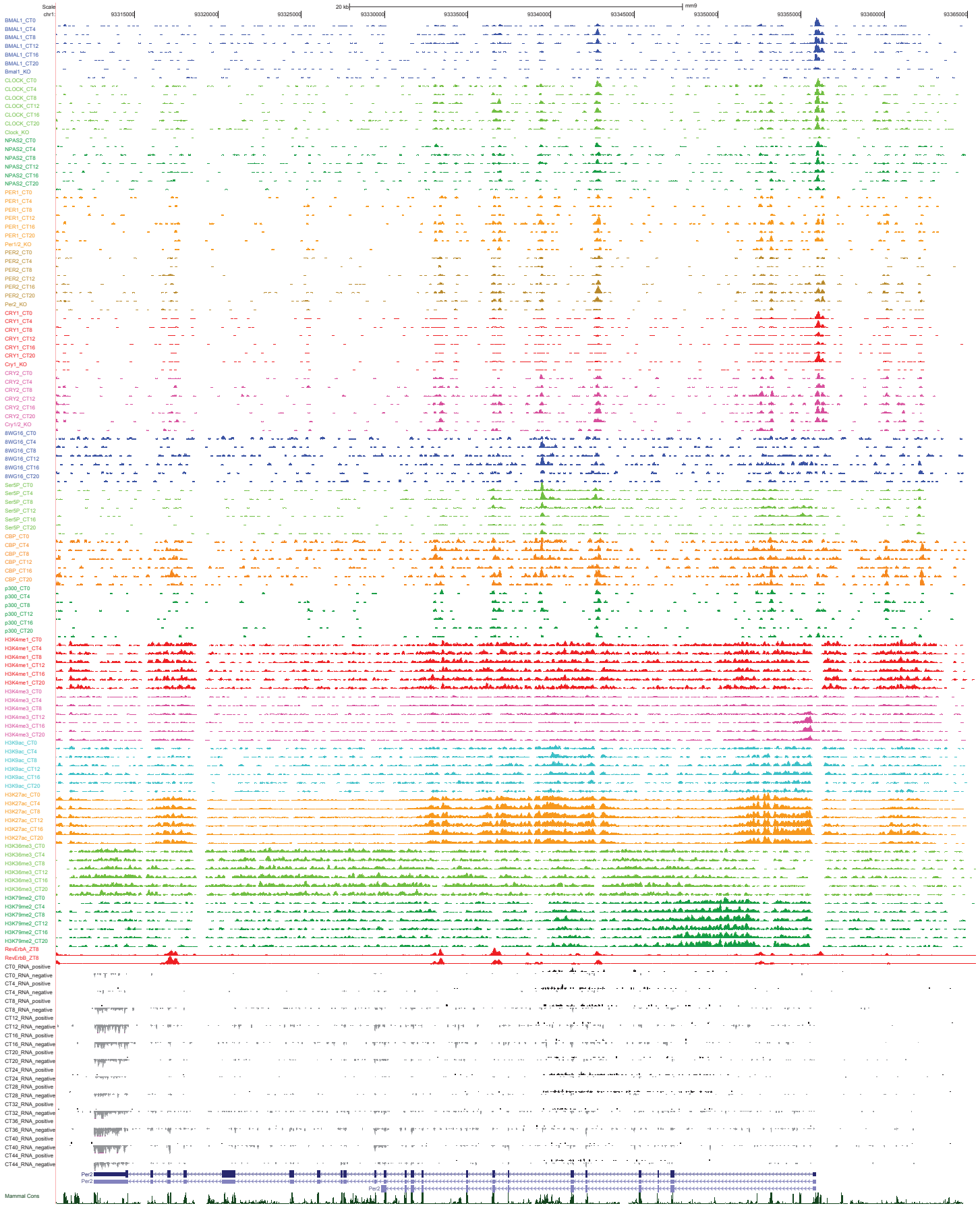
Scale
chr1:
20 kb
mm9
93315000
93320000
93325000
93330000
93335000
93340000
93345000
93350000
93355000
93360000
93365000
BMAL1_CT0
BMAL1_CT4
BMAL1_CT8
BMAL1_CT12
BMAL1_CT16
BMAL1_CT20
Bmal1_KO
CLOCK_CT0
CLOCK_CT4
CLOCK_CT8
CLOCK_CT12
CLOCK_CT16
CLOCK_CT20
Clock_KO
NPAS2_CT0
NPAS2_CT4
NPAS2_CT8
NPAS2_CT12
NPAS2_CT16
NPAS2_CT20
PER1_CT0
PER1_CT4
PER1_CT8
PER1_CT12
PER1_CT16
PER1_CT20
Per1/2_KO
PER2_CT0
PER2_CT4
PER2_CT8
PER2_CT12
PER2_CT16
PER2_CT20
Per2_KO
CRY1_CT0
CRY1_CT4
CRY1_CT8
CRY1_CT12
CRY1_CT16
CRY1_CT20
Cry1_KO
CRY2_CT0
CRY2_CT4
CRY2_CT8
CRY2_CT12
CRY2_CT16
CRY2_CT20
Cry1/2_KO
BWG16_CT0
BWG16_CT4
BWG16_CT8
BWG16_CT12
BWG16_CT16
BWG16_CT20
Ser5P_CT0
Ser5P_CT4
Ser5P_CT8
Ser5P_CT12
Ser5P_CT16
Ser5P_CT20
CBP_CT0
CBP_CT4
CBP_CT8
CBP_CT12
CBP_CT16
CBP_CT20
p300_CT0
p300_CT4
p300_CT8
p300_CT12
p300_CT16
p300_CT20
H3K4me1_CT0
H3K4me1_CT4
H3K4me1_CT8
H3K4me1_CT12
H3K4me1_CT16
H3K4me1_CT20
H3K4me3_CT0
H3K4me3_CT4
H3K4me3_CT8
H3K4me3_CT12
H3K4me3_CT16
H3K4me3_CT20
H3K9ac_CT0
H3K9ac_CT4
H3K9ac_CT8
H3K9ac_CT12
H3K9ac_CT16
H3K9ac_CT20
H3K27ac_CT0
H3K27ac_CT4
H3K27ac_CT8
H3K27ac_CT12
H3K27ac_CT16
H3K27ac_CT20
H3K36me3_CT0
H3K36me3_CT4
H3K36me3_CT8
H3K36me3_CT12
H3K36me3_CT16
H3K36me3_CT20
H3K79me2_CT0
H3K79me2_CT4
H3K79me2_CT8
H3K79me2_CT12
H3K79me2_CT16
H3K79me2_CT20
RevErbA_ZT8
RevErbB_ZT8
CT0_RNA_positive
CT0_RNA_negative
CT4_RNA_positive
CT4_RNA_negative
CT8_RNA_positive
CT8_RNA_negative
CT12_RNA_positive
CT12_RNA_negative
CT16_RNA_positive
CT16_RNA_negative
CT20_RNA_positive
CT20_RNA_negative
CT24_RNA_positive
CT24_RNA_negative
CT28_RNA_positive
CT28_RNA_negative
CT32_RNA_positive
CT32_RNA_negative
CT36_RNA_positive
CT36_RNA_negative
CT40_RNA_positive
CT40_RNA_negative
CT44_RNA_positive
CT44_RNA_negative
Per2
Per2
Per2
Mammal Cons

G

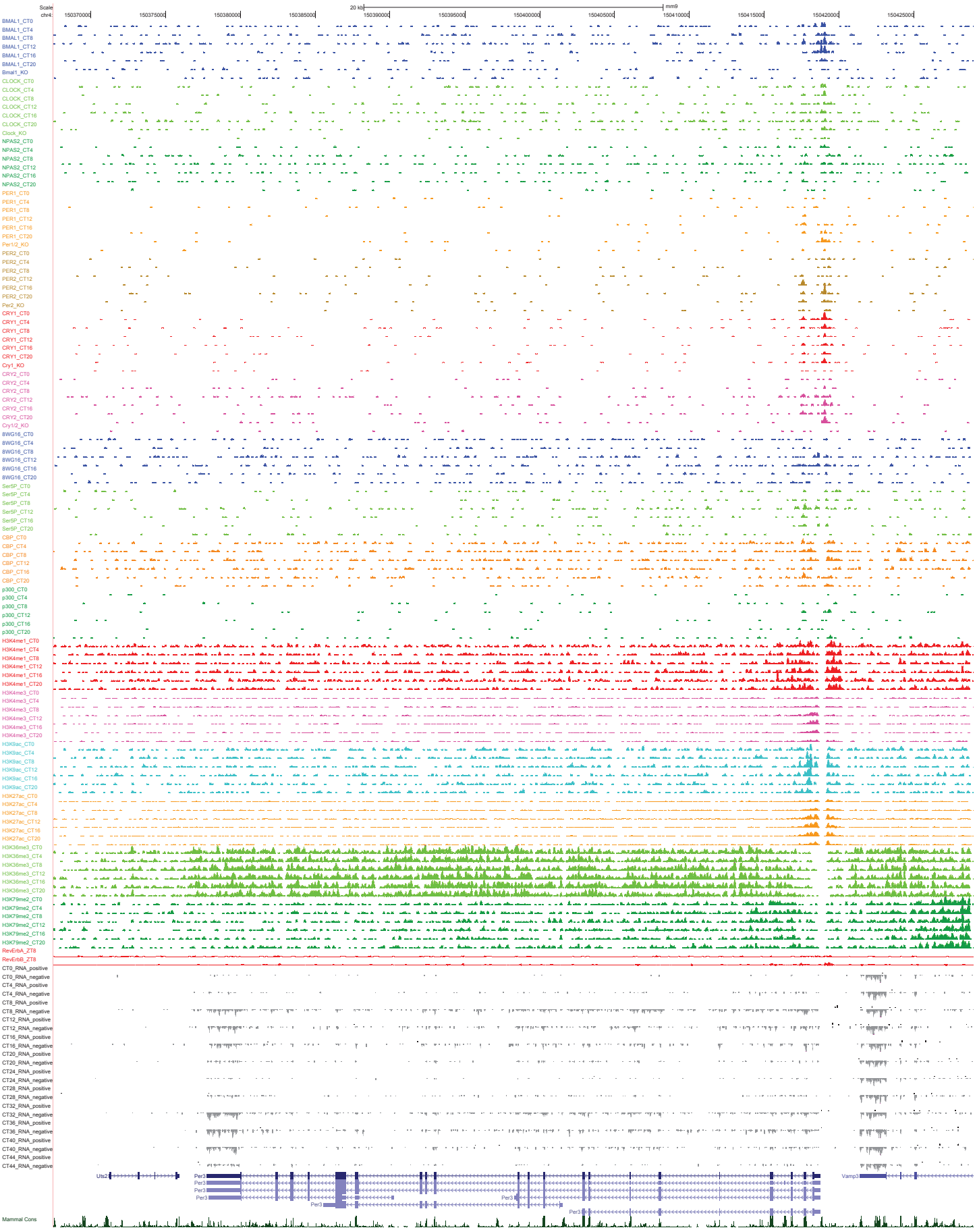
Scale
chr4:
20 kb
mm9
150370000
150375000
150380000
150385000
150390000
150395000
150400000
150405000
150410000
150415000
150420000
150425000
BMAL1_CT0
BMAL1_CT4
BMAL1_CT8
BMAL1_CT12
BMAL1_CT16
BMAL1_CT20
Bmal1_KO
CLOCK_CT0
CLOCK_CT4
CLOCK_CT8
CLOCK_CT12
CLOCK_CT16
CLOCK_CT20
Clock_KO
NPAS2_CT0
NPAS2_CT4
NPAS2_CT8
NPAS2_CT12
NPAS2_CT16
NPAS2_CT20
PER1_CT0
PER1_CT4
PER1_CT8
PER1_CT12
PER1_CT16
PER1_CT20
Per1/2_KO
PER2_CT0
PER2_CT4
PER2_CT8
PER2_CT12
PER2_CT16
PER2_CT20
Per2_KO
CRY1_CT0
CRY1_CT4
CRY1_CT8
CRY1_CT12
CRY1_CT16
CRY1_CT20
Cry1_KO
CRY2_CT0
CRY2_CT4
CRY2_CT8
CRY2_CT12
CRY2_CT16
CRY2_CT20
Cry1/2_KO
BWG16_CT0
BWG16_CT4
BWG16_CT8
BWG16_CT12
BWG16_CT16
BWG16_CT20
Ser5P_CT0
Ser5P_CT4
Ser5P_CT8
Ser5P_CT12
Ser5P_CT16
Ser5P_CT20
CBP_CT0
CBP_CT4
CBP_CT8
CBP_CT12
CBP_CT16
CBP_CT20
p300_CT0
p300_CT4
p300_CT8
p300_CT12
p300_CT16
p300_CT20
H3K4me1_CT0
H3K4me1_CT4
H3K4me1_CT8
H3K4me1_CT12
H3K4me1_CT16
H3K4me1_CT20
H3K4me3_CT0
H3K4me3_CT4
H3K4me3_CT8
H3K4me3_CT12
H3K4me3_CT16
H3K4me3_CT20
H3K9ac_CT0
H3K9ac_CT4
H3K9ac_CT8
H3K9ac_CT12
H3K9ac_CT16
H3K9ac_CT20
H3K27ac_CT0
H3K27ac_CT4
H3K27ac_CT8
H3K27ac_CT12
H3K27ac_CT16
H3K27ac_CT20
H3K36me3_CT0
H3K36me3_CT4
H3K36me3_CT8
H3K36me3_CT12
H3K36me3_CT16
H3K36me3_CT20
H3K79me2_CT0
H3K79me2_CT4
H3K79me2_CT8
H3K79me2_CT12
H3K79me2_CT16
H3K79me2_CT20
RevErbA_ZT8
RevErbB_ZT8
CT0_RNA_positive
CT0_RNA_negative
CT4_RNA_positive
CT4_RNA_negative
CT8_RNA_positive
CT8_RNA_negative
CT12_RNA_positive
CT12_RNA_negative
CT16_RNA_positive
CT16_RNA_negative
CT20_RNA_positive
CT20_RNA_negative
CT24_RNA_positive
CT24_RNA_negative
CT28_RNA_positive
CT28_RNA_negative
CT32_RNA_positive
CT32_RNA_negative
CT36_RNA_positive
CT36_RNA_negative
CT40_RNA_positive
CT40_RNA_negative
CT44_RNA_positive
CT44_RNA_negative
Uts2
Per3
Vamp3
Mammal Cons

H

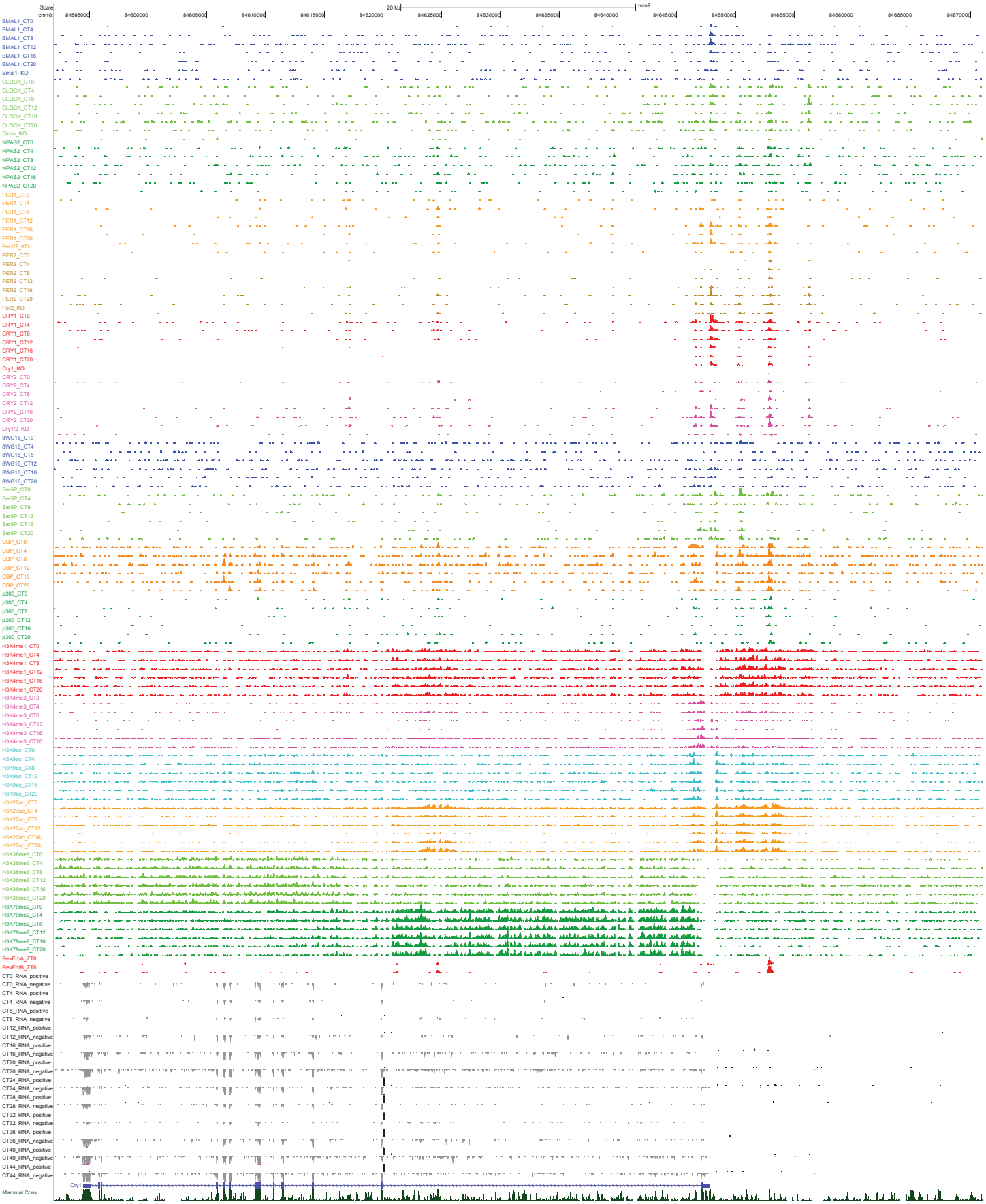
Scale
chr10:
84595000
84600000
84605000
84610000
84615000
20 kb
84620000
84625000
84630000
84635000
84640000
mm9
84645000
84650000
84655000
84660000
84665000
84670000
BMAL1_CT0
BMAL1_CT4
BMAL1_CT8
BMAL1_CT12
BMAL1_CT16
BMAL1_CT20
Bmal1_KO
CLOCK_CT0
CLOCK_CT4
CLOCK_CT8
CLOCK_CT12
CLOCK_CT16
CLOCK_CT20
Clock_KO
NPAS2_CT0
NPAS2_CT4
NPAS2_CT8
NPAS2_CT12
NPAS2_CT16
NPAS2_CT20
PER1_CT0
PER1_CT4
PER1_CT8
PER1_CT12
PER1_CT16
PER1_CT20
Per1/2_KO
PER2_CT0
PER2_CT4
PER2_CT8
PER2_CT12
PER2_CT16
PER2_CT20
Per2_KO
CRY1_CT0
CRY1_CT4
CRY1_CT8
CRY1_CT12
CRY1_CT16
CRY1_CT20
Cry1_KO
CRY2_CT0
CRY2_CT4
CRY2_CT8
CRY2_CT12
CRY2_CT16
CRY2_CT20
Cry1/2_KO
BWG16_CT0
BWG16_CT4
BWG16_CT8
BWG16_CT12
BWG16_CT16
BWG16_CT20
Ser5P_CT0
Ser5P_CT4
Ser5P_CT8
Ser5P_CT12
Ser5P_CT16
Ser5P_CT20
CBP_CT0
CBP_CT4
CBP_CT8
CBP_CT12
CBP_CT16
CBP_CT20
p300_CT0
p300_CT4
p300_CT8
p300_CT12
p300_CT16
p300_CT20
H3K4me1_CT0
H3K4me1_CT4
H3K4me1_CT8
H3K4me1_CT12
H3K4me1_CT16
H3K4me1_CT20
H3K4me3_CT0
H3K4me3_CT4
H3K4me3_CT8
H3K4me3_CT12
H3K4me3_CT16
H3K4me3_CT20
H3K9ac_CT0
H3K9ac_CT4
H3K9ac_CT8
H3K9ac_CT12
H3K9ac_CT16
H3K9ac_CT20
H3K27ac_CT0
H3K27ac_CT4
H3K27ac_CT8
H3K27ac_CT12
H3K27ac_CT16
H3K27ac_CT20
H3K36me3_CT0
H3K36me3_CT4
H3K36me3_CT8
H3K36me3_CT12
H3K36me3_CT16
H3K36me3_CT20
H3K79me2_CT0
H3K79me2_CT4
H3K79me2_CT8
H3K79me2_CT12
H3K79me2_CT16
H3K79me2_CT20
RevErbA_ZT8
RevErbB_ZT8
CT0_RNA_positive
CT0_RNA_negative
CT4_RNA_positive
CT4_RNA_negative
CT8_RNA_positive
CT8_RNA_negative
CT12_RNA_positive
CT12_RNA_negative
CT16_RNA_positive
CT16_RNA_negative
CT20_RNA_positive
CT20_RNA_negative
CT24_RNA_positive
CT24_RNA_negative
CT28_RNA_positive
CT28_RNA_negative
CT32_RNA_positive
CT32_RNA_negative
CT36_RNA_positive
CT36_RNA_negative
CT40_RNA_positive
CT40_RNA_negative
CT44_RNA_positive
CT44_RNA_negative
Cry1
Mammal Cons

I


Scale
chr2:
20 kb
mm9
9223500
9224000
9224500
9225000
9225500
9226000
9226500
9227000
9227500
9228000
9228500
BMAL1_CT0
BMAL1_CT4
BMAL1_CT8
BMAL1_CT12
BMAL1_CT16
BMAL1_CT20
Bmal1_KO
CLOCK_CT0
CLOCK_CT4
CLOCK_CT8
CLOCK_CT12
CLOCK_CT16
CLOCK_CT20
Clock_KO
NPAS2_CT0
NPAS2_CT4
NPAS2_CT8
NPAS2_CT12
NPAS2_CT16
NPAS2_CT20
PER1_CT0
PER1_CT4
PER1_CT8
PER1_CT12
PER1_CT16
PER1_CT20
Per1/2_KO
PER2_CT0
PER2_CT4
PER2_CT8
PER2_CT12
PER2_CT16
PER2_CT20
Per2_KO
CRY1_CT0
CRY1_CT4
CRY1_CT8
CRY1_CT12
CRY1_CT16
CRY1_CT20
Cry1_KO
CRY2_CT0
CRY2_CT4
CRY2_CT8
CRY2_CT12
CRY2_CT16
CRY2_CT20
Cry1/2_KO
BWG16_CT0
BWG16_CT4
BWG16_CT8
BWG16_CT12
BWG16_CT16
BWG16_CT20
Ser5P_CT0
Ser5P_CT4
Ser5P_CT8
Ser5P_CT12
Ser5P_CT16
Ser5P_CT20
CBP_CT0
CBP_CT4
CBP_CT8
CBP_CT12
CBP_CT16
CBP_CT20
p300_CT0
p300_CT4
p300_CT8
p300_CT12
p300_CT16
p300_CT20
H3K4me1_CT0
H3K4me1_CT4
H3K4me1_CT8
H3K4me1_CT12
H3K4me1_CT16
H3K4me1_CT20
H3K4me3_CT0
H3K4me3_CT4
H3K4me3_CT8
H3K4me3_CT12
H3K4me3_CT16
H3K4me3_CT20
H3K9ac_CT0
H3K9ac_CT4
H3K9ac_CT8
H3K9ac_CT12
H3K9ac_CT16
H3K9ac_CT20
H3K27ac_CT0
H3K27ac_CT4
H3K27ac_CT8
H3K27ac_CT12
H3K27ac_CT16
H3K27ac_CT20
H3K36me3_CT0
H3K36me3_CT4
H3K36me3_CT8
H3K36me3_CT12
H3K36me3_CT16
H3K36me3_CT20
H3K79me2_CT0
H3K79me2_CT4
H3K79me2_CT8
H3K79me2_CT12
H3K79me2_CT16
H3K79me2_CT20
RevErbA_ZT8
RevErbB_ZT8
CT0_RNA_positive
CT0_RNA_negative
CT4_RNA_positive
CT4_RNA_negative
CT8_RNA_positive
CT8_RNA_negative
CT12_RNA_positive
CT12_RNA_negative
CT16_RNA_positive
CT16_RNA_negative
CT20_RNA_positive
CT20_RNA_negative
CT24_RNA_positive
CT24_RNA_negative
CT28_RNA_positive
CT28_RNA_negative
CT32_RNA_positive
CT32_RNA_negative
CT36_RNA_positive
CT36_RNA_negative
CT40_RNA_positive
CT40_RNA_negative
CT44_RNA_positive
CT44_RNA_negative
Mapk8ip1
Mapk8ip1
Mapk8ip1
Cry2
Cry2
mPHLL2
Mammal Cons

J

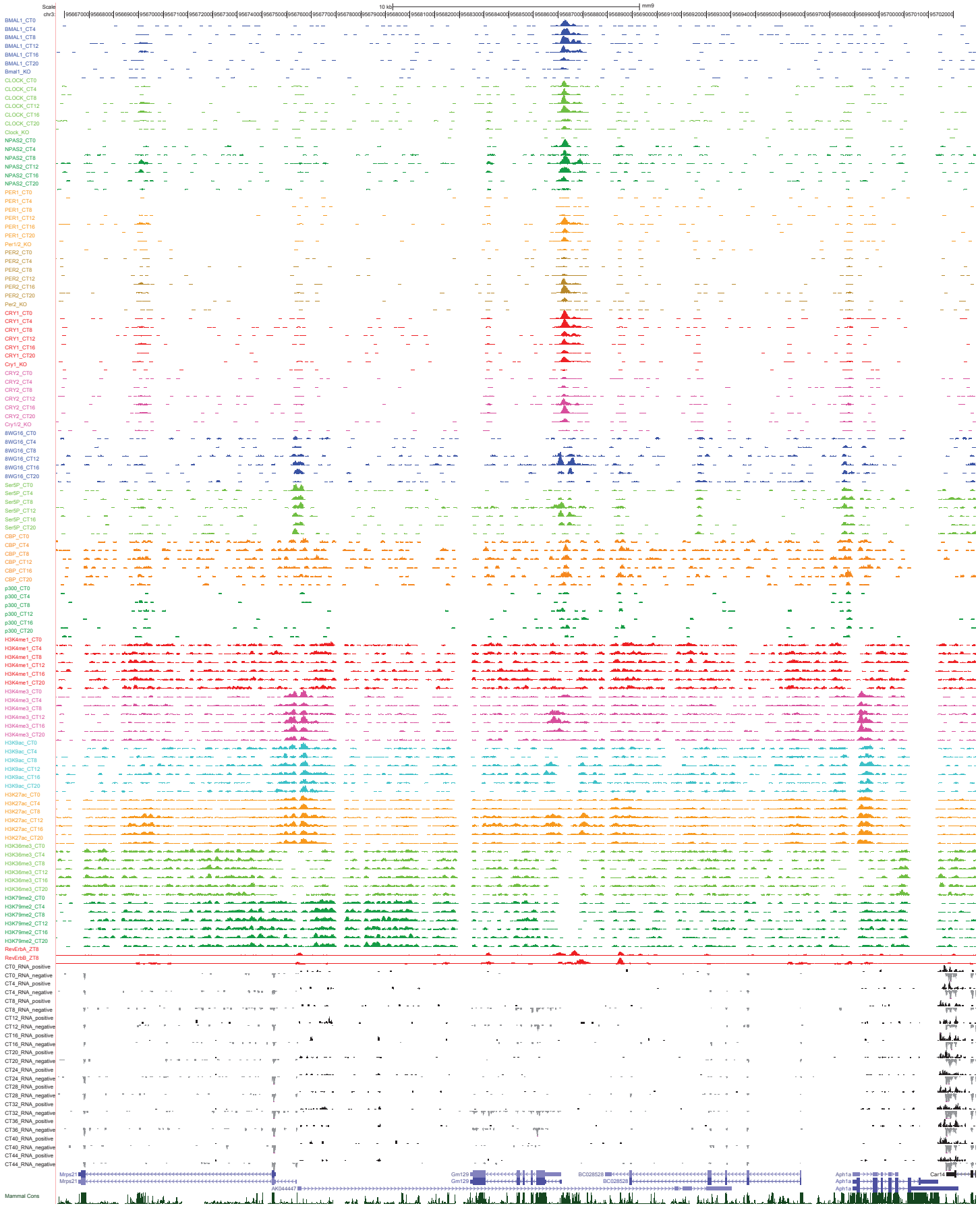
Scale
chr3:
10 kb
mm9
BMAL1_CT0
BMAL1_CT4
BMAL1_CT8
BMAL1_CT12
BMAL1_CT16
BMAL1_CT20
Bmal1_KO
CLOCK_CT0
CLOCK_CT4
CLOCK_CT8
CLOCK_CT12
CLOCK_CT16
CLOCK_CT20
Clock_KO
NPAS2_CT0
NPAS2_CT4
NPAS2_CT8
NPAS2_CT12
NPAS2_CT16
NPAS2_CT20
PER1_CT0
PER1_CT4
PER1_CT8
PER1_CT12
PER1_CT16
PER1_CT20
Per1/2_KO
PER2_CT0
PER2_CT4
PER2_CT8
PER2_CT12
PER2_CT16
PER2_CT20
Per2_KO
CRY1_CT0
CRY1_CT4
CRY1_CT8
CRY1_CT12
CRY1_CT16
CRY1_CT20
Cry1_KO
CRY2_CT0
CRY2_CT4
CRY2_CT8
CRY2_CT12
CRY2_CT16
CRY2_CT20
Cry1/2_KO
BWG16_CT0
BWG16_CT4
BWG16_CT8
BWG16_CT12
BWG16_CT16
BWG16_CT20
Ser5P_CT0
Ser5P_CT4
Ser5P_CT8
Ser5P_CT12
Ser5P_CT16
Ser5P_CT20
CBP_CT0
CBP_CT4
CBP_CT8
CBP_CT12
CBP_CT16
CBP_CT20
p300_CT0
p300_CT4
p300_CT8
p300_CT12
p300_CT16
p300_CT20
H3K4me1_CT0
H3K4me1_CT4
H3K4me1_CT8
H3K4me1_CT12
H3K4me1_CT16
H3K4me1_CT20
H3K4me3_CT0
H3K4me3_CT4
H3K4me3_CT8
H3K4me3_CT12
H3K4me3_CT16
H3K4me3_CT20
H3K9ac_CT0
H3K9ac_CT4
H3K9ac_CT8
H3K9ac_CT12
H3K9ac_CT16
H3K9ac_CT20
H3K27ac_CT0
H3K27ac_CT4
H3K27ac_CT8
H3K27ac_CT12
H3K27ac_CT16
H3K27ac_CT20
H3K36me3_CT0
H3K36me3_CT4
H3K36me3_CT8
H3K36me3_CT12
H3K36me3_CT16
H3K36me3_CT20
H3K79me2_CT0
H3K79me2_CT4
H3K79me2_CT8
H3K79me2_CT12
H3K79me2_CT16
H3K79me2_CT20
RevErbA_ZT8
RevErbB_ZT8
CT0_RNA_positive
CT0_RNA_negative
CT4_RNA_positive
CT4_RNA_negative
CT8_RNA_positive
CT8_RNA_negative
CT12_RNA_positive
CT12_RNA_negative
CT16_RNA_positive
CT16_RNA_negative
CT20_RNA_positive
CT20_RNA_negative
CT24_RNA_positive
CT24_RNA_negative
CT28_RNA_positive
CT28_RNA_negative
CT32_RNA_positive
CT32_RNA_negative
CT36_RNA_positive
CT36_RNA_negative
CT40_RNA_positive
CT40_RNA_negative
CT44_RNA_positive
CT44_RNA_negative
Mrps21
Mrps21
Gm129
Gm129
BC028528
BC028528
Aph1a
Aph1a
Aph1a
Car14
AK044447
Mammal Cons

K

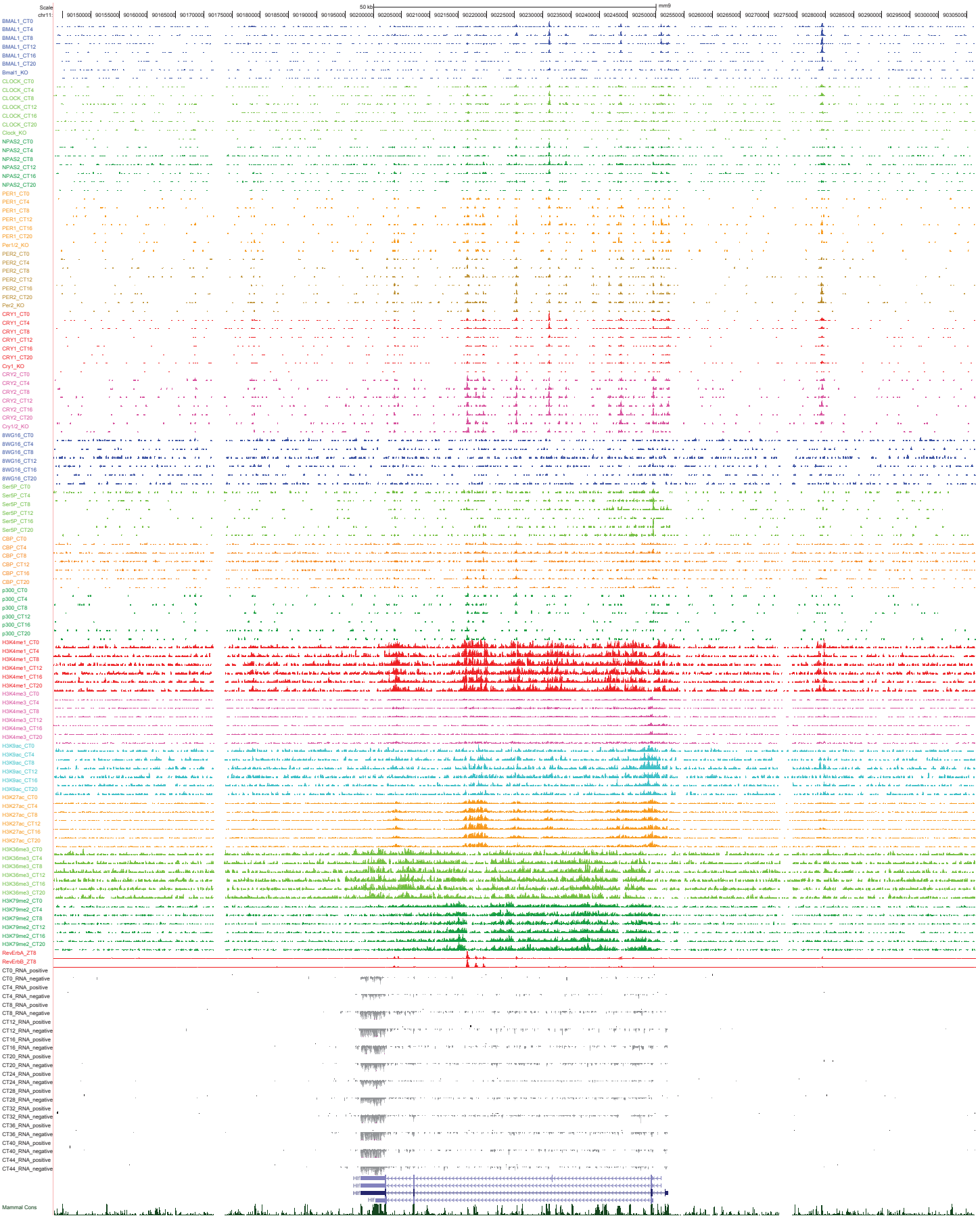
Scale
chr11:
50 kb
mm9
BMAL1_CT0
BMAL1_CT4
BMAL1_CT8
BMAL1_CT12
BMAL1_CT16
BMAL1_CT20
Bmal1_KO
CLOCK_CT0
CLOCK_CT4
CLOCK_CT8
CLOCK_CT12
CLOCK_CT16
CLOCK_CT20
Clock_KO
NPAS2_CT0
NPAS2_CT4
NPAS2_CT8
NPAS2_CT12
NPAS2_CT16
NPAS2_CT20
PER1_CT0
PER1_CT4
PER1_CT8
PER1_CT12
PER1_CT16
PER1_CT20
Per1/2_KO
PER2_CT0
PER2_CT4
PER2_CT8
PER2_CT12
PER2_CT16
PER2_CT20
Per2_KO
CRY1_CT0
CRY1_CT4
CRY1_CT8
CRY1_CT12
CRY1_CT16
CRY1_CT20
Cry1_KO
CRY2_CT0
CRY2_CT4
CRY2_CT8
CRY2_CT12
CRY2_CT16
CRY2_CT20
Cry1/2_KO
8WG16_CT0
8WG16_CT4
8WG16_CT8
8WG16_CT12
8WG16_CT16
8WG16_CT20
Ser5P_CT0
Ser5P_CT4
Ser5P_CT8
Ser5P_CT12
Ser5P_CT16
Ser5P_CT20
CBP_CT0
CBP_CT4
CBP_CT8
CBP_CT12
CBP_CT16
CBP_CT20
p300_CT0
p300_CT4
p300_CT8
p300_CT12
p300_CT16
p300_CT20
H3K4me1_CT0
H3K4me1_CT4
H3K4me1_CT8
H3K4me1_CT12
H3K4me1_CT16
H3K4me1_CT20
H3K4me3_CT0
H3K4me3_CT4
H3K4me3_CT8
H3K4me3_CT12
H3K4me3_CT16
H3K4me3_CT20
H3K9ac_CT0
H3K9ac_CT4
H3K9ac_CT8
H3K9ac_CT12
H3K9ac_CT16
H3K9ac_CT20
H3K27ac_CT0
H3K27ac_CT4
H3K27ac_CT8
H3K27ac_CT12
H3K27ac_CT16
H3K27ac_CT20
H3K36me3_CT0
H3K36me3_CT4
H3K36me3_CT8
H3K36me3_CT12
H3K36me3_CT16
H3K36me3_CT20
H3K79me2_CT0
H3K79me2_CT4
H3K79me2_CT8
H3K79me2_CT12
H3K79me2_CT16
H3K79me2_CT20
RevErbA_ZT8
RevErbB_ZT8
CT0_RNA_positive
CT0_RNA_negative
CT4_RNA_positive
CT4_RNA_negative
CT8_RNA_positive
CT8_RNA_negative
CT12_RNA_positive
CT12_RNA_negative
CT16_RNA_positive
CT16_RNA_negative
CT20_RNA_positive
CT20_RNA_negative
CT24_RNA_positive
CT24_RNA_negative
CT28_RNA_positive
CT28_RNA_negative
CT32_RNA_positive
CT32_RNA_negative
CT36_RNA_positive
CT36_RNA_negative
CT40_RNA_positive
CT40_RNA_negative
CT44_RNA_positive
CT44_RNA_negative
Hif
Hif
Hif
Hif
Mammal Cons

L

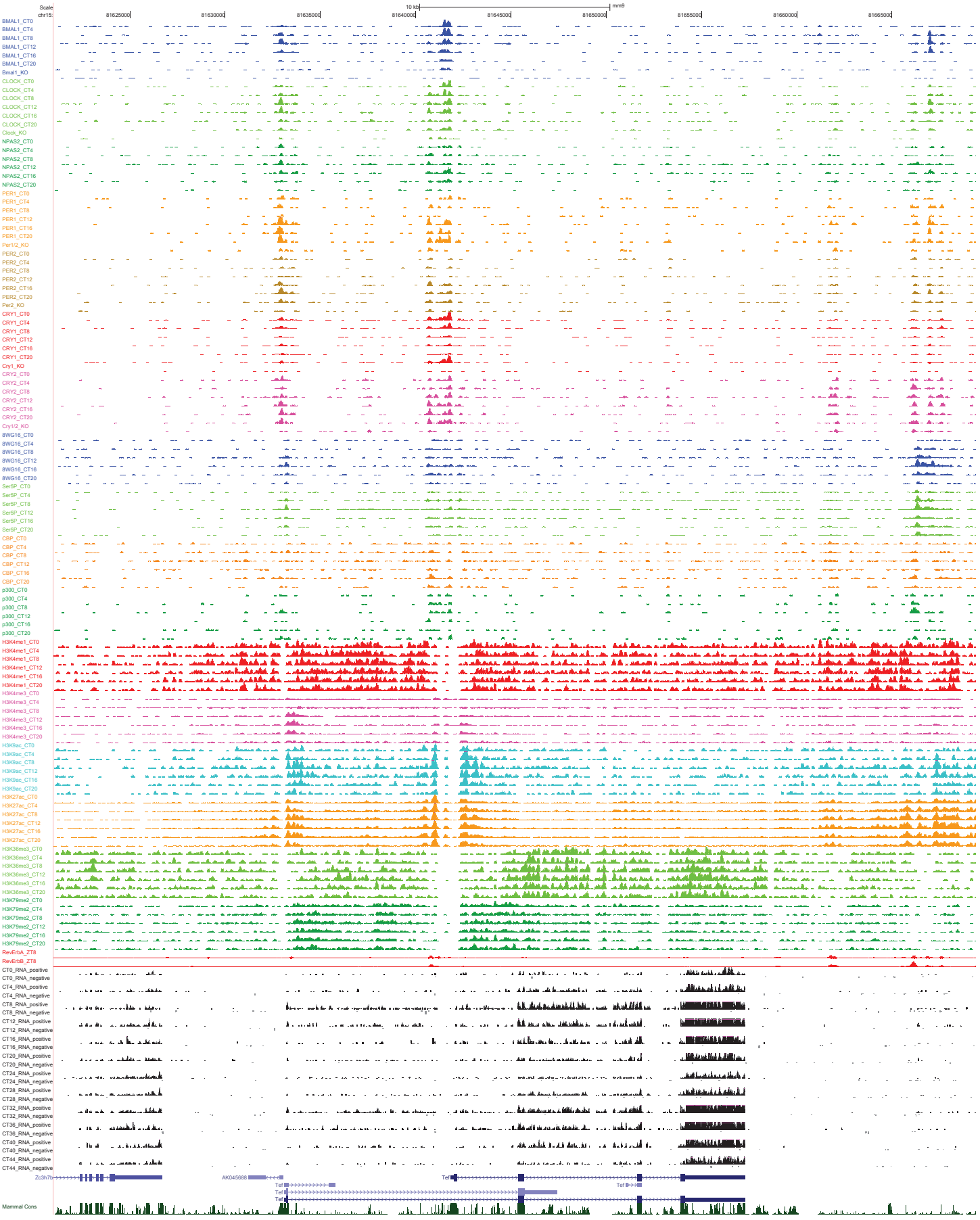
Scale
chr15:
81625000
81630000
81635000
10 kb
81640000
81645000
81650000
mm9
81655000
81660000
81665000
BMAL1_CT0
BMAL1_CT4
BMAL1_CT8
BMAL1_CT12
BMAL1_CT16
BMAL1_CT20
Bmal1_KO
CLOCK_CT0
CLOCK_CT4
CLOCK_CT8
CLOCK_CT12
CLOCK_CT16
CLOCK_CT20
Clock_KO
NPAS2_CT0
NPAS2_CT4
NPAS2_CT8
NPAS2_CT12
NPAS2_CT16
NPAS2_CT20
PER1_CT0
PER1_CT4
PER1_CT8
PER1_CT12
PER1_CT16
PER1_CT20
Per1/2_KO
PER2_CT0
PER2_CT4
PER2_CT8
PER2_CT12
PER2_CT16
PER2_CT20
Per2_KO
CRY1_CT0
CRY1_CT4
CRY1_CT8
CRY1_CT12
CRY1_CT16
CRY1_CT20
Cry1_KO
CRY2_CT0
CRY2_CT4
CRY2_CT8
CRY2_CT12
CRY2_CT16
CRY2_CT20
Cry1/2_KO
BWG16_CT0
BWG16_CT4
BWG16_CT8
BWG16_CT12
BWG16_CT16
BWG16_CT20
Ser5P_CT0
Ser5P_CT4
Ser5P_CT8
Ser5P_CT12
Ser5P_CT16
Ser5P_CT20
CBP_CT0
CBP_CT4
CBP_CT8
CBP_CT12
CBP_CT16
CBP_CT20
p300_CT0
p300_CT4
p300_CT8
p300_CT12
p300_CT16
p300_CT20
H3K4me1_CT0
H3K4me1_CT4
H3K4me1_CT8
H3K4me1_CT12
H3K4me1_CT16
H3K4me1_CT20
H3K4me3_CT0
H3K4me3_CT4
H3K4me3_CT8
H3K4me3_CT12
H3K4me3_CT16
H3K4me3_CT20
H3K9ac_CT0
H3K9ac_CT4
H3K9ac_CT8
H3K9ac_CT12
H3K9ac_CT16
H3K9ac_CT20
H3K27ac_CT0
H3K27ac_CT4
H3K27ac_CT8
H3K27ac_CT12
H3K27ac_CT16
H3K27ac_CT20
H3K36me3_CT0
H3K36me3_CT4
H3K36me3_CT8
H3K36me3_CT12
H3K36me3_CT16
H3K36me3_CT20
H3K79me2_CT0
H3K79me2_CT4
H3K79me2_CT8
H3K79me2_CT12
H3K79me2_CT16
H3K79me2_CT20
RevErbA_ZT8
RevErbB_ZT8
CT0_RNA_positive
CT0_RNA_negative
CT4_RNA_positive
CT4_RNA_negative
CT8_RNA_positive
CT8_RNA_negative
CT12_RNA_positive
CT12_RNA_negative
CT16_RNA_positive
CT16_RNA_negative
CT20_RNA_positive
CT20_RNA_negative
CT24_RNA_positive
CT24_RNA_negative
CT28_RNA_positive
CT28_RNA_negative
CT32_RNA_positive
CT32_RNA_negative
CT36_RNA_positive
CT36_RNA_negative
CT40_RNA_positive
CT40_RNA_negative
CT44_RNA_positive
CT44_RNA_negative
Zc3h7b
AK045688
Tef
Tef
Tef
Tef
Mammal Cons

M

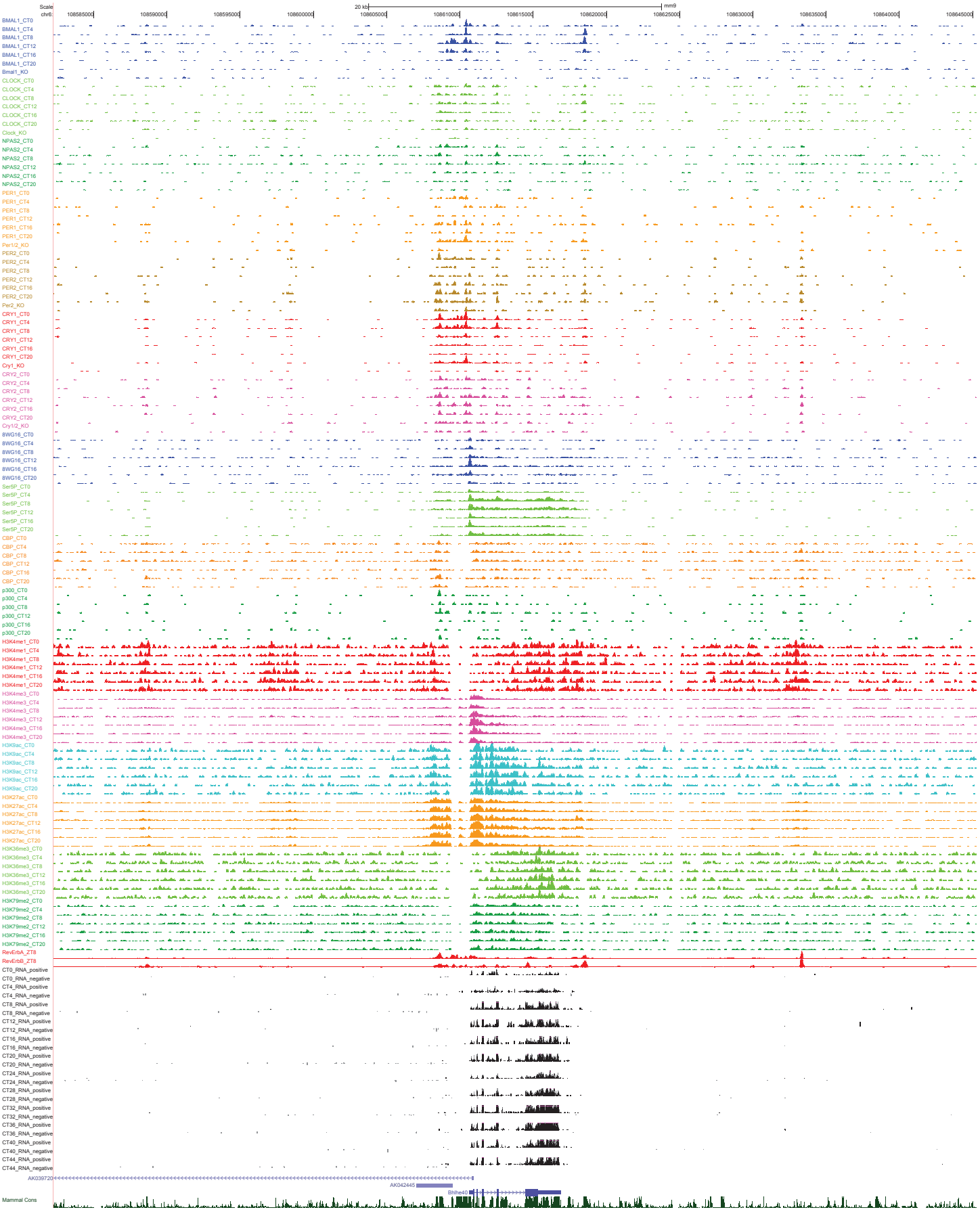
Scale
chr6:
108585000
108590000
108595000
108600000
20 kb
108605000
108610000
108615000
108620000
108625000
mm9
108630000
108635000
108640000
108645000
BMAL1_CT0
BMAL1_CT4
BMAL1_CT8
BMAL1_CT12
BMAL1_CT16
BMAL1_CT20
Bmal1_KO
CLOCK_CT0
CLOCK_CT4
CLOCK_CT8
CLOCK_CT12
CLOCK_CT16
CLOCK_CT20
Clock_KO
NPAS2_CT0
NPAS2_CT4
NPAS2_CT8
NPAS2_CT12
NPAS2_CT16
NPAS2_CT20
PER1_CT0
PER1_CT4
PER1_CT8
PER1_CT12
PER1_CT16
PER1_CT20
Per1/2_KO
PER2_CT0
PER2_CT4
PER2_CT8
PER2_CT12
PER2_CT16
PER2_CT20
Per2_KO
CRY1_CT0
CRY1_CT4
CRY1_CT8
CRY1_CT12
CRY1_CT16
CRY1_CT20
Cry1_KO
CRY2_CT0
CRY2_CT4
CRY2_CT8
CRY2_CT12
CRY2_CT16
CRY2_CT20
Cry1/2_KO
BWG16_CT0
BWG16_CT4
BWG16_CT8
BWG16_CT12
BWG16_CT16
BWG16_CT20
Ser5P_CT0
Ser5P_CT4
Ser5P_CT8
Ser5P_CT12
Ser5P_CT16
Ser5P_CT20
CBP_CT0
CBP_CT4
CBP_CT8
CBP_CT12
CBP_CT16
CBP_CT20
p300_CT0
p300_CT4
p300_CT8
p300_CT12
p300_CT16
p300_CT20
H3K4me1_CT0
H3K4me1_CT4
H3K4me1_CT8
H3K4me1_CT12
H3K4me1_CT16
H3K4me1_CT20
H3K4me3_CT0
H3K4me3_CT4
H3K4me3_CT8
H3K4me3_CT12
H3K4me3_CT16
H3K4me3_CT20
H3K9ac_CT0
H3K9ac_CT4
H3K9ac_CT8
H3K9ac_CT12
H3K9ac_CT16
H3K9ac_CT20
H3K27ac_CT0
H3K27ac_CT4
H3K27ac_CT8
H3K27ac_CT12
H3K27ac_CT16
H3K27ac_CT20
H3K36me3_CT0
H3K36me3_CT4
H3K36me3_CT8
H3K36me3_CT12
H3K36me3_CT16
H3K36me3_CT20
H3K79me2_CT0
H3K79me2_CT4
H3K79me2_CT8
H3K79me2_CT12
H3K79me2_CT16
H3K79me2_CT20
RevErbA_ZT8
RevErbB_ZT8
CT0_RNA_positive
CT0_RNA_negative
CT4_RNA_positive
CT4_RNA_negative
CT8_RNA_positive
CT8_RNA_negative
CT12_RNA_positive
CT12_RNA_negative
CT16_RNA_positive
CT16_RNA_negative
CT20_RNA_positive
CT20_RNA_negative
CT24_RNA_positive
CT24_RNA_negative
CT28_RNA_positive
CT28_RNA_negative
CT32_RNA_positive
CT32_RNA_negative
CT36_RNA_positive
CT36_RNA_negative
CT40_RNA_positive
CT40_RNA_negative
CT44_RNA_positive
CT44_RNA_negative
AK039720
AK042445
Bhlhe40
Mammal Cons

N

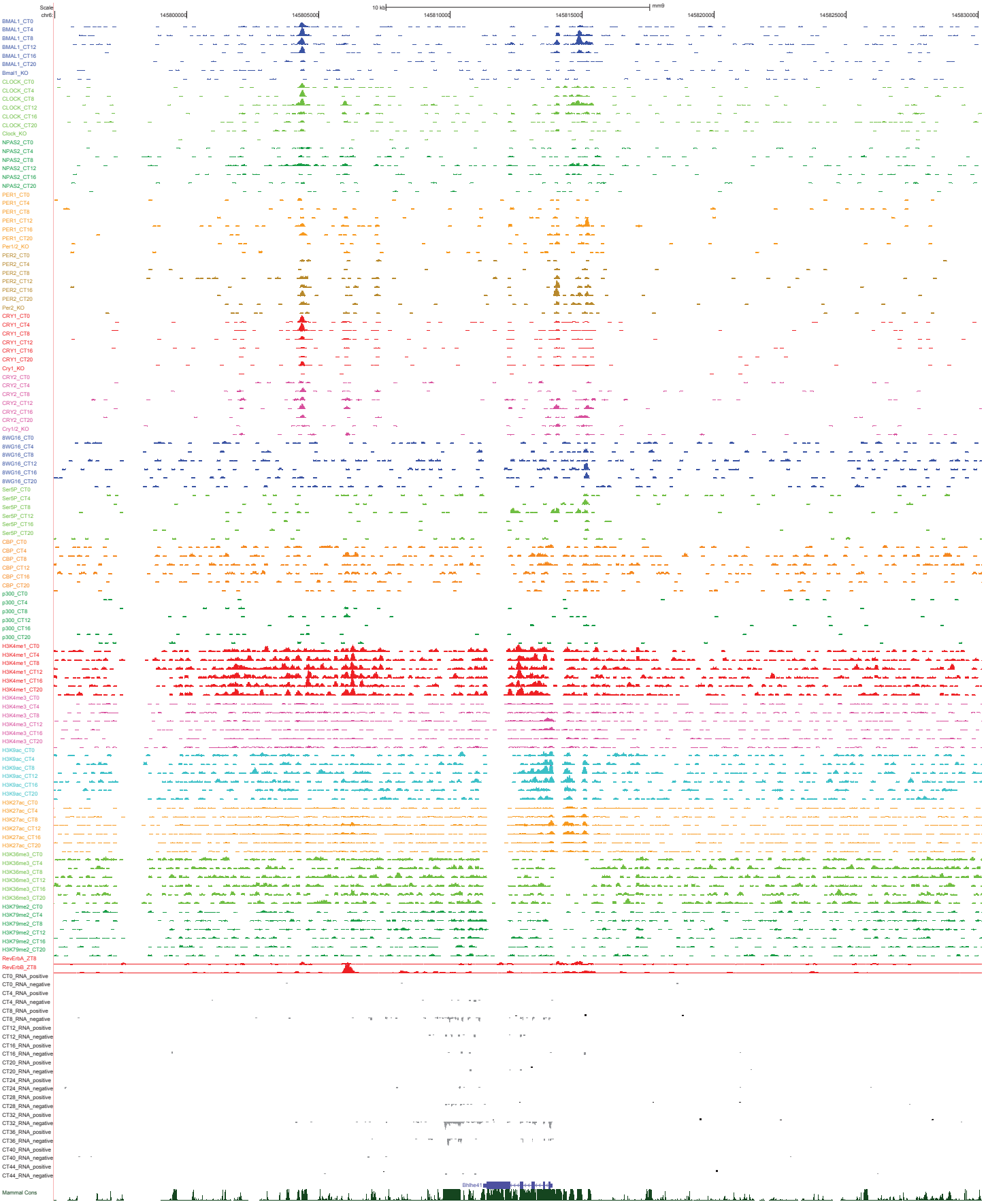
Scale
chr6
10 kb
mm9
145800000
145805000
145810000
145815000
145820000
145825000
145830000
BMAL1_CT0
BMAL1_CT4
BMAL1_CT8
BMAL1_CT12
BMAL1_CT16
BMAL1_CT20
Bmal1_KO
CLOCK_CT0
CLOCK_CT4
CLOCK_CT8
CLOCK_CT12
CLOCK_CT16
CLOCK_CT20
Clock_KO
NPAS2_CT0
NPAS2_CT4
NPAS2_CT8
NPAS2_CT12
NPAS2_CT16
NPAS2_CT20
PER1_CT0
PER1_CT4
PER1_CT8
PER1_CT12
PER1_CT16
PER1_CT20
Per1/2_KO
PER2_CT0
PER2_CT4
PER2_CT8
PER2_CT12
PER2_CT16
PER2_CT20
Per2_KO
CRY1_CT0
CRY1_CT4
CRY1_CT8
CRY1_CT12
CRY1_CT16
CRY1_CT20
Cry1_KO
CRY2_CT0
CRY2_CT4
CRY2_CT8
CRY2_CT12
CRY2_CT16
CRY2_CT20
Cry1/2_KO
8WG16_CT0
8WG16_CT4
8WG16_CT8
8WG16_CT12
8WG16_CT16
8WG16_CT20
Ser5P_CT0
Ser5P_CT4
Ser5P_CT8
Ser5P_CT12
Ser5P_CT16
Ser5P_CT20
CBP_CT0
CBP_CT4
CBP_CT8
CBP_CT12
CBP_CT16
CBP_CT20
p300_CT0
p300_CT4
p300_CT8
p300_CT12
p300_CT16
p300_CT20
H3K4me1_CT0
H3K4me1_CT4
H3K4me1_CT8
H3K4me1_CT12
H3K4me1_CT16
H3K4me1_CT20
H3K4me3_CT0
H3K4me3_CT4
H3K4me3_CT8
H3K4me3_CT12
H3K4me3_CT16
H3K4me3_CT20
H3K9ac_CT0
H3K9ac_CT4
H3K9ac_CT8
H3K9ac_CT12
H3K9ac_CT16
H3K9ac_CT20
H3K27ac_CT0
H3K27ac_CT4
H3K27ac_CT8
H3K27ac_CT12
H3K27ac_CT16
H3K27ac_CT20
H3K36me3_CT0
H3K36me3_CT4
H3K36me3_CT8
H3K36me3_CT12
H3K36me3_CT16
H3K36me3_CT20
H3K79me2_CT0
H3K79me2_CT4
H3K79me2_CT8
H3K79me2_CT12
H3K79me2_CT16
H3K79me2_CT20
RevErbA_ZT8
RevErbB_ZT8
CT0_RNA_positive
CT0_RNA_negative
CT4_RNA_positive
CT4_RNA_negative
CT8_RNA_positive
CT8_RNA_negative
CT12_RNA_positive
CT12_RNA_negative
CT16_RNA_positive
CT16_RNA_negative
CT20_RNA_positive
CT20_RNA_negative
CT24_RNA_positive
CT24_RNA_negative
CT28_RNA_positive
CT28_RNA_negative
CT32_RNA_positive
CT32_RNA_negative
CT36_RNA_positive
CT36_RNA_negative
CT40_RNA_positive
CT40_RNA_negative
CT44_RNA_positive
CT44_RNA_negative
Bhlhe41
Mammal Cons